In vivo applications of bioorthogonal reactions- chemistry and targeting mechanisms

Mitry, Madonna M. A., Greco, Francesca and Osborn, Helen M. I. (2023) In vivo applications of bioorthogonal reactions-chemistry and targeting mechanisms. Chemistry - A European Journal, 29 (20). e202203942. ISSN 0947-6539 doi: https://doi.org/10.1002/chem.202203942 Available at https://centaur.reading.ac.uk/109958/

Chemistry Europe
European Chemical Societies Publishing

WILEY VCH

Excellence in Chemistry Research

Announcing our new flagship journal

- Gold Open Access
- Publishing charges waived
- Preprints welcome
- Edited by active scientists

Meet the Editors of *ChemistryEurope*

Luisa De Cola
Università degli Studi di Milano Statale, Italy

Ive Hermans
University of Wisconsin-Madison, USA

Ken Tanaka
Tokyo Institute of Technology, Japan

Chemistry–A European Journal
Review
doi.org/10.1002/chem.202203942
Chemistry Europe
European Chemical Societies Publishing

www.chemeurj.org

In Vivo Applications of Bioorthogonal Reactions: Chemistry and Targeting Mechanisms

Madonna M. A. Mitry,[a, b] Francesca Greco,*[a] and Helen M. I. Osborn*[a]

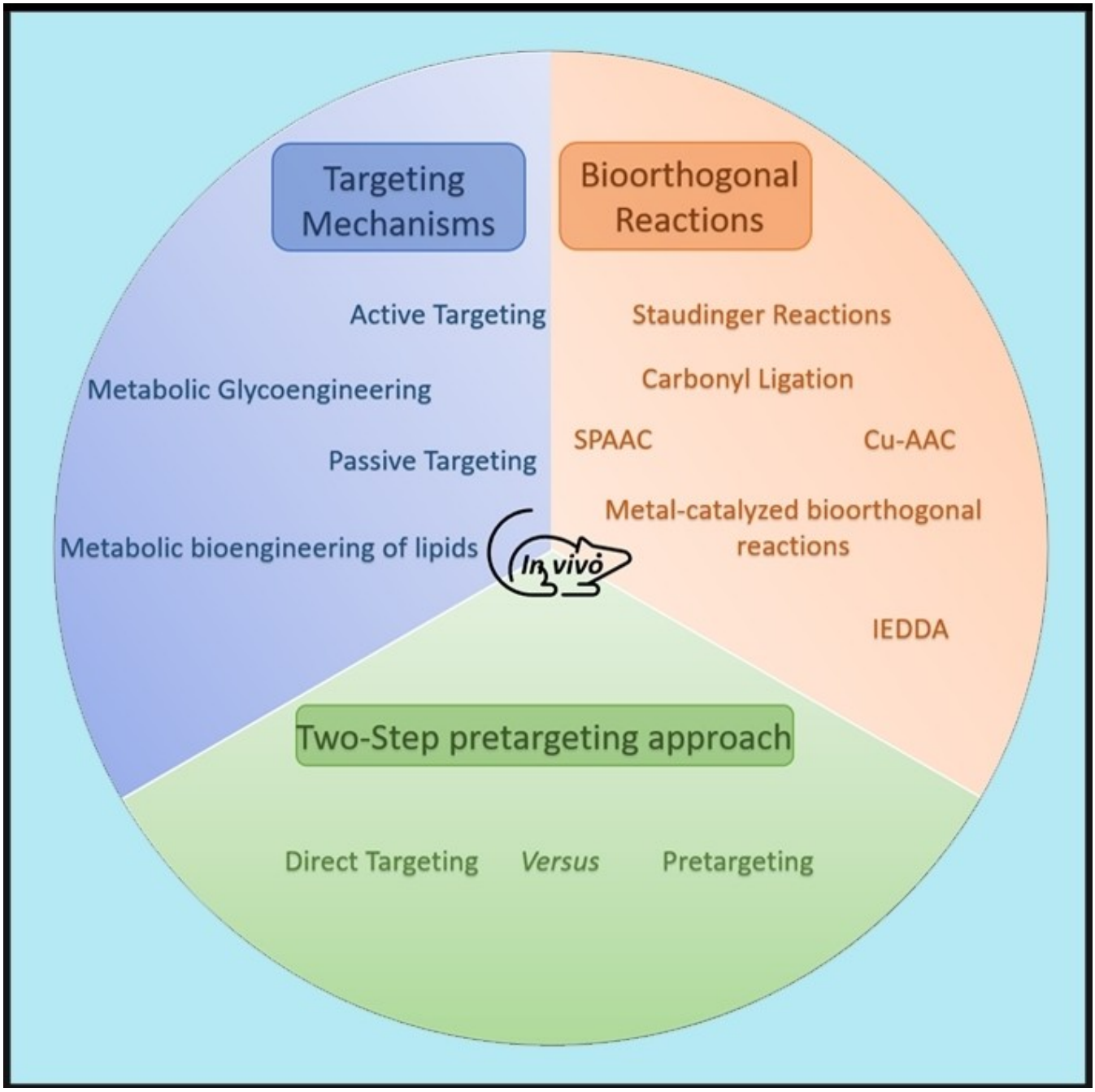

Abstract: Bioorthogonal chemistry involves selective biocompatible reactions between functional groups that are not normally present in biology. It has been used to probe biomolecules in living systems, and has advanced biomedical strategies such as diagnostics and therapeutics. In this review, the challenges and opportunities encountered when translating *in vitro* bioorthogonal approaches to *in vivo* settings are presented, with a focus on methods to deliver the bioorthogonal reaction components. These methods include metabolic bioengineering, active targeting, passive targeting, and simultaneously used strategies. The suitability of bioorthogonal ligation reactions and bond cleavage reactions for *in vivo* applications is critically appraised, and practical considerations such as the optimum scheduling regimen in pretargeting approaches are discussed. Finally, we present our own perspectives for this area and identify what, in our view, are the key challenges that must be overcome to maximise the impact of these approaches.

1. Introduction

Bioorthogonal chemistry involves selective chemical reactions between functional groups that are not normally present in biological systems. In the last two decades, this approach has revolutionised the study of biomolecules in their native environment, has advanced imaging and diagnosis strategies, and has afforded drug delivery strategies for living cells.[1–9] To be effective *in vivo*, and hence maximise the clinical impact of the approach, it is essential that the reactions proceed at relatively fast reaction rates under physiological conditions.[10,11] Moreover, the bioorthogonal moieties must be nontoxic and stable *in vivo*.[12,13] As a consequence of these challenges, fewer *in vivo* applications of bioorthogonal reactions have been reported compared with *in vitro* applications. Those that have been reported focus on the labelling of biomolecules for imaging purposes, tracking the *in vivo* journey of cell therapeutics in regenerative medicine, targeted drug delivery, and in-situ prodrug activation.

Many excellent reviews detail the types of bioorthogonal reactions developed so far,[11,14–16] and their *in vitro* applications, with a focus on diagnosis[17] and therapy.[18] Recent bioorthogonal chemistry strategies to image and detect biomolecules in intracellular compartments have also been reviewed.[19] In this complementary review, we focus specifically on the *in vivo* applications of bioorthogonal reactions of therapeutic relevance, and uncouple the different elements that lead to a promising bioorthogonal-based application in biological systems. First, the development of bioorthogonal reactions, and their suitability for translation to *in vivo* settings, are discussed (Section 2). Second, the targeting mechanisms used to deliver the bioorthogonal components are classified and their effectiveness are discussed (Section 3). Then, Section 4 investigates the scheduling approaches that have been proposed for delivering the two bioorthogonal reaction components (pretargeting approach) for radiolabelling. Finally, in Section 5, we present our own perspectives for this area and identify what, in our view, are the key challenges that must be overcome to maximise the impact of these approaches.

[a] *M. M. A. Mitry, Prof. F. Greco, Prof. H. M. I. Osborn*
Reading School of Pharmacy, University of Reading
Whiteknights, Reading, RG6 6AD (UK)
E-mail: f.greco@reading.ac.uk
h.m.i.osborn@reading.ac.uk

[b] *M. M. A. Mitry*
Department of Pharmaceutical Chemistry
Faculty of Pharmacy, Ain Shams University
Cairo 11566 (Egypt)

2. Bioorthogonal Reactions

Bioorthogonal chemistry is a term that was first introduced by Bertozzi[20] in 2003 to refer to chemical reactions that can proceed under physiological conditions without interfering with biological processes and biomolecules. Before 2003, bioorthogonal reactions were often classified as chemoselective ligation reactions involving, for example, carbonyl ligations,[21–23] the Staudinger ligation,[24,25] 1,3-dipolar cycloadditions,[26] thioesters[27] and thioethers.[28] These advances were underpinned by work from the 1990s, where chemical ligation (also known as orthogonal reactions) was reported as an evolving novel synthetic strategy for the construction of proteins and multimeric protein assemblies from unprotected peptide fragments in aqueous solution through multiple bioorthogonal reactions.[29–31]

Over the past 20 years, bioorthogonal chemistry has continued to facilitate many significant advances in chemical biology for example by allowing biomolecules to be studied in their native environment.[10,11,14–16,32] Herein we discuss and critically appraise the bioorthogonal reactions that are reported to be successfully used *in vivo*, and provide the context for the development by highlighting the key milestones in the development of each reaction.

2.1. Staudinger reactions

The Staudinger ligation was one of the first reported bioorthogonal reactions. It originates from the classical Staudinger reaction between an azide and triphenylphosphine that progresses via an unstable iminophosphorane intermediate to afford amine and phosphine oxide products (Figure 1). In 2000, Bertozzi reported the modified reaction, the Staudinger ligation,

for selective ligation of two molecules.[25] Thus, introduction of an electrophilic trap (usually an acyl group) onto the phosphine moiety captures the iminophosphorane intermediate and subsequent hydrolysis then forms an amide bond between the two reactants. In the same year, Bertozzi[24] and Raines[33] simultaneously reported a further Staudinger ligation reaction called the traceless Staudinger ligation for chemoselective synthesis of amide bonds. A cleavable linkage is added between the phosphine and the electrophilic trap such that cleavage of the iminophosphorane transfers the acyl group to the azide bearing molecule to form a stable amide bond (Figure 1).

Additional developments have also allowed prodrug activation, for example in 2006 Azoulay et al.[34] reported the release of doxorubicin from a carbamate-linked doxorubicin/triphenylphosphine prodrug through a rearrangement of the azaylide intermediate formed during the Staudinger ligation. In 2008, Brakel et al.[35] also reported a Staudinger reaction-mediated release of doxorubicin from a prodrug through a complementary mechanism (Figure 1). The doxorubicin was linked to the azide trigger instead of the phosphine by a carbamate linker and the release mechanism involved the reduction of the azide into an amine through its reaction with the triphenylphosphine activator which leads to a 1,6-elimination drug release mechanism.

Staudinger ligation is advantageous in terms of its high selectivity between the azide and phosphine. In terms of the biocompatibility, the azide is a small and biocompatible functional group and the intramolecular cyclisation step is fast and durable with complex biomolecules in aqueous environment making it a good candidate for use in living systems applications.[36] However, the main limitation for its applications *in vivo* is its slow kinetics ($k = 10^{-3}\,M^{-1}\,s^{-1}$) which mean that high concentrations of both reactants are needed. Also, the phosphines are prone to oxidation under physiological conditions making control of their concentration *in vivo* very challenging.

In 2017, Ramström and Yan[37] reported a development of the Staudinger ligation using perfluoroaryl azides (PFAAs) that can react with triarylphosphines to afford stable, nonhydrolysed iminophosphorane intermediates hence removing the need for electrophilic traps. This reaction has improved kinetics with a rate constant of $18\,M^{-1}\,s^{-1}$.

The applications of Staudinger reactions have been widely reported in chemical biology research including peptide synthesis,[33] cell imaging,[38–40] antigen cross-presentation[41] and controlling protein function[42,43] analysis.[44] Staudinger ligation was first applied *in vivo* to prove the validity of metabolic glycan engineering (MGE) in living animals using Ac_4ManNAz to introduce the azide on cell surfaces' glycans.[45] A light-activated Staudinger – Bertozzi reagent has also been developed in an approach to photocage the phosphine moiety and prevent its oxidation until it reaches the desired site of action.[46] Recently, nanocarriers modified with triphenylphosphine side chains that carry active drugs that react with engineered azide reporters on the surface of tumour cells have been reported for *in vivo* tumour targeting.[47]

2.2. Carbonyl ligation

Carbonyl ligations involve condensation of hydrazines or hydroxylamines with aldehydes or ketones to form oximes or hydrazones (Figure 2). In vitro, the reaction was reported for developing a strategy to study carbohydrate-mediated cell surface interactions[48] and small-molecule drug delivery.[22,49] It has also been used in protein synthesis,[21] protein labelling,[50] BR96-doxorubicin immunoconjugates synthesis for doxorubicin release in tumour lysosomes[51] and 3D *in vitro* tissue structure model generation.[52]

Although both aldehydes and ketones can be introduced to cell surfaces to serve as an anchor for *in vivo* bioorthogonal ligations, ketones are generally preferred as they are more inert towards biomolecules. However, they bring the disadvantage of being less reactive than aldehydes. Translation of carbonyl

Madonna M. A. Mitry received her B.Sc. and M.Sc. degrees in medicinal chemistry from Ain Shams University in Cairo in 2018. She is currently working as a PhD student in the School of Pharmacy at the University of Reading, UK. Her research focuses on the design of prodrugs that are activated by bioorthogonal reactions for selective cancer treatment.

Francesca Greco obtained her degree in pharmaceutical chemistry and technologies from the University of Pisa in 2002, with her masters thesis done at Pharmacia (Nerviano, Milan, later part of Pfizer). She then did a PhD in drug delivery (2002–2006) at Cardiff University, under the supervision of Profs. Ruth Duncan and Rob Nicholson. After finishing her PhD, Francesca was appointed to the University of Reading, where she is now Professor of Pharmaceutics. Her works focuses on drug delivery, in particular through polymer–drug conjugates.

Helen M.I. Osborn obtained her degree in chemistry from the University of Oxford in 1991, and her PhD in synthetic and biological chemistry from the University of Bristol, supervised by Professor Sweeney, in 1994. She then completed post-doctoral research in carbohydrate chemistry at the University of Cambridge, with Professor Ley. Helen joined the University of Reading in 1996 and is currently Professor of Biomedicinal Chemistry. Her research develops selective medicinal chemistry strategies using prodrugs and carbohydrate-based therapeutics.

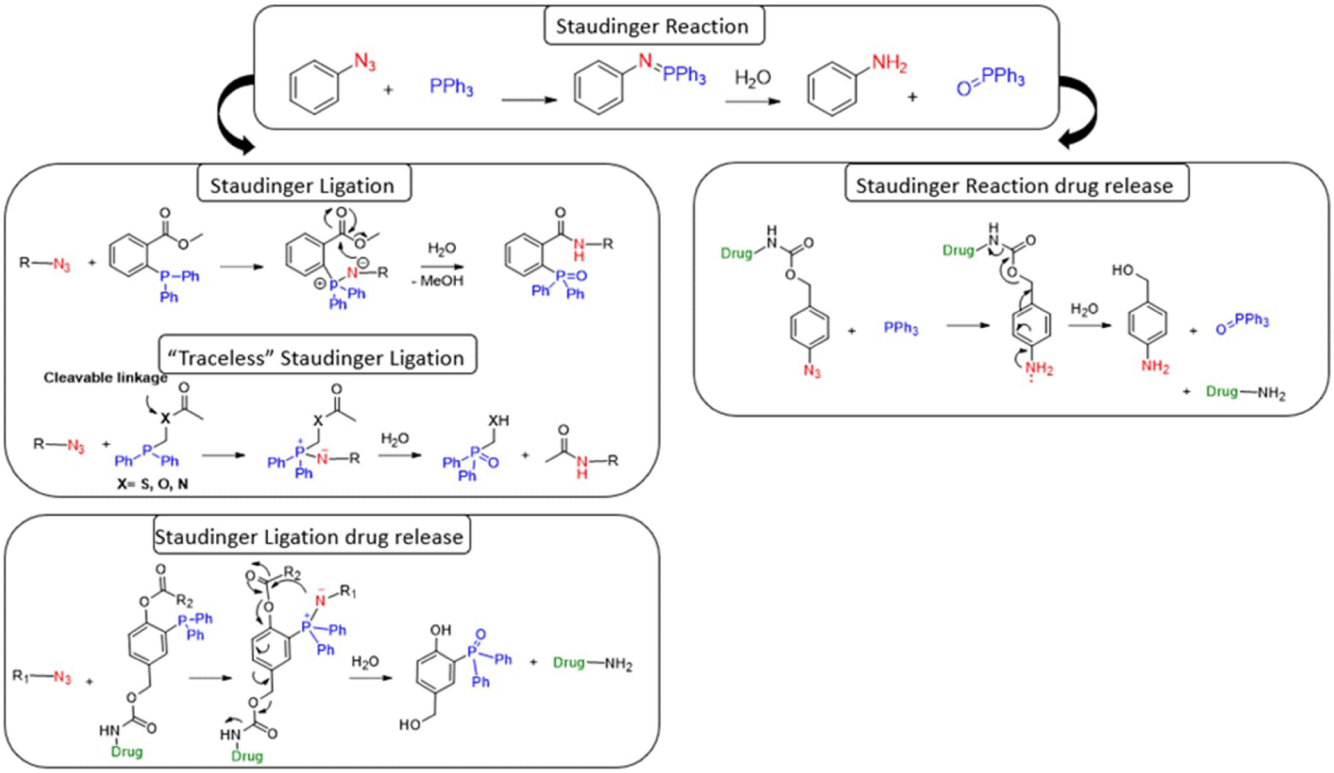

Figure 1. Summary of Staudinger reactions.

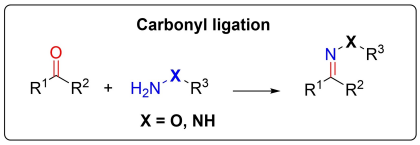

Figure 2. Carbonyl ligation reactions.

ligations to *in vivo* settings poses further challenges as the overall reaction kinetics under physiological conditions are very slow, due to acidic conditions being required for better ligation rates. Also, although oximes are more stable than hydrazones to hydrolysis at physiological pH, the products are all susceptible to hydrolysis in aqueous media. Furthermore, the reactions are limited to the cell surface as aldehydes and ketones are prone to intracellular metabolism. Catalysts such as aniline,[53] saline[54] and *m*-phenylenediamine[55] and *ortho* substitutions on the aromatic carbonyl ring like halogens[56] and boronic acid[57] were reported to be used to increase the reaction rate *in vitro*.

Due to these challenges, *in vivo* oxime ligation has not been widely investigated. However, it has proved successful for targeted cancer treatment approaches where *O*-dodecyloxyamine has been successfully encapsulated in liposomes to label cancer cells with the oxyamine functional group allowing subsequent targeting with aldehyde-modified nanoparticles.[58]

2.3. Azide-alkyne cycloadditions reactions

Cycloaddition reactions between azides (1,3-dipole) and alkynes (dipolarophile) to produce a 1,2,3-triazole are classified into two groups of reactions, the copper-catalysed azide-alkyne cycloaddition (CuAAC) and the strain-promoted azide-alkyne cycloaddition (SPAAC)(Figure 3).

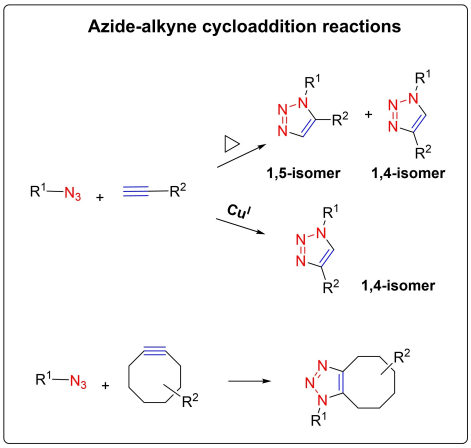

Figure 3. Azide-alkyne cycloaddition reactions.

2.3.1. Copper-catalysed azide-alkyne cycloaddition

The mechanism and kinetics of 1,3-dipolar cycloadditions were extensively studied and reported by Huisgen in 1963.[59] The uncatalysed reaction kinetics are slow under physiological conditions and need elevated temperatures which lead to the formation of two regioisomers. Meldal[60] and Sharpless[26] reported in 2002 that the addition of a Cu^{I} catalyst increases the reaction kinetics and regioselectivity, introducing the concept of click chemistry.

The toxicity of reactive oxygen species (ROS) produced by the copper catalyst makes the CuAAC reaction less suitable for biological applications. In living systems, the Cu^{I} is oxidised to Cu^{II} in a redox cycle consuming ascorbates that generates ROS causing oxidative degradation of proteins and peptides with different extents.[61,62] To address this, auxiliary triazole-based ligands[63] such as tri-(triazolylmethyl)amines have been developed to decrease the Cu^{I} concentration and hence the oxidative stress level in living cells, allowing successful *in vivo* imaging of glycans.[64] A complementary strategy to protect the cells from ROS damage has been developed by Ting et al. in which the azide contains an internal pyridylmethyl azide copper-chelating moiety which acts as a sacrificial reductant during site-specific labelling of cell-surface proteins.[65] Recently, Qu et al. reported the development of a heterogeneous copper catalyst on a metal-organic framework that can accumulate preferably at the mitochondria for in-situ site-specific drug synthesis in mitochondria This has been applied *in vivo* for the localised synthesis of resveratrol-derived drugs for tumour therapy.[66] Entrapment of the copper catalyst in nanoparticles has also resulted in decreased copper toxicity[67] and these have been used to catalyse the in-situ synthesis of combretastatin A4 from azide and alkyne precursors both *in vitro* and *in vivo* where a zebrafish model demonstrated its biocompatibility.

2.3.2. Strain-promoted azide-alkyne cycloaddition (SPAAC)

SPAAC is a Cu-free click reaction established by Bertozzi in 2004[68] to improve the slow kinetics of the uncatalysed azide-alkyne cycloaddition and remove the potentially toxic copper catalyst. The slow rate of the reaction and the high concentrations of the bioorthogonal components required initially hampered progress in this area (CuAAC $k \sim 10^{1}\,M^{-1}s^{-1}$, SPAAC $k \sim 10^{-3}\,M^{-1}s^{-1}$). However, incorporation of electron withdrawing substituents such as fluorine,[69–71] fused rings, and nitrogen-containing rings including 4-dibenzocyclooctynols DIBO,[72] bicyclononynes BCN[73] and aza-dibenzocyclooctynes DIBAC[74] increased the ring strain and thereby increased the reaction rate ($k \sim 10^{-1}\,M^{-1}s^{-1}$). SPAAC reactions have been one of the mostly commonly used bioorthogonal reactions for modification and imaging of biomolecules in living cells due to their high selectivity and the availability of azide-modified monosaccharide precursors for efficient cellular expression of the azide functional group which can be subsequently reacted with a strained alkyne that is attached to a fluorescent dye.[69,73,75] Conjugation of dibenzocyclooctyne (DBCO) or azadibenzocyclooctyne (ADIBO) to florescent dyes has enabled live tracking of exosomes,[76] chondrocytes[77] and cell therapeutics[78] that have engineered azide groups on their surface, *in vivo*. Conjugation of DBCO to a targeting peptide such as the dimeric NGR peptide, and an azide to a fluorescent dye, has also facilitated tumour imaging *in vivo*.[79]

2.4. Cycloaddition of azide and *trans*-cyclooctene (TCO)

The 1,3-dipolar cycloaddition between an azide and TCO, to form a highly unstable triazoline product that rearranges after loss of nitrogen to give an aldimine, ketimine and aziridine, was first reported in 1992 by Shea.[80] Gamble et al. hypothesised that the imine intermediates could be used for prodrug activation, by hydrolysis and 1,6-elimination, when attached to an electron-deficient linker. This activation mechanism was validated *in vitro* for prodrug activation where an azide-doxorubicin prodrug was activated by *trans*-cyclooctene in melanoma cells restoring doxorubicin's cytotoxicity.[81] Protein activation through *trans*-cyclooctene activation of *p*-azidobenzyloxycarbonyl lysine in HEK293T cells[82] also validated the mechanism. In vivo, a *p*-azidobenzylcarbamate doxorubicin prodrug was successfully activated at the tumour site after tumour pretargeting of a functionalised TCO appended to cetuximab-EGFR Ab in a murine melanoma mice model[83] (Figure 4).

2.5. Metal-catalysed bioorthogonal reactions

Palladium-mediated ligation of biomolecules was first reported in 2006 for protein modification;[84–87] tuning of the palladium catalyst to optimise the rate of the reaction has also been reviewed.[14,16] Palladium-mediated bond cleavage has also been widely used, due to the specificity and chemical stability of the transition metal catalysts, to deprotect amino and hydroxyl groups allowing prodrug and protein deprotection and bioactivation in living cells[32,88,89] (Figure 5). For example Bradley et al. have reported the development of palladium nanoparticles trapped within polystyrene microspheres that can enter the cell in order to mediate allylcarbamate cleavage and Suzuki-Miyaura cross-coupling reactions. These have facilitated cellular labelling, and synthesis of modulators or inhibitors of cell function.[90] In vivo applications of Pd-mediated reactions have been hindered due to concerns about tissue accumulation, stability, solubility and toxicity. However, they have been reported for in-situ prodrug activation where the Pd complex can be encapsulated in a nanoparticle that accumulates at the tumour site due to the enhanced permeability and retention (EPR) effect, hence minimising the systemic distribution to off-target tissues. Weissler et al. reported the usage of a nanoformulation of bis[tri(2-furyl)phosphine]palladium(II) dichloride ($PdCl_2(TFP)_2$)-PEG for allylcarbamate cleavage allowing the activation of an allyloxycarbonyl-caged doxorubicin prodrug and a bis(allyloxycarbamate)-caged rhodamine-110 fluorophore.[91] Wu et al. reported the use of a Pd–ferrocene

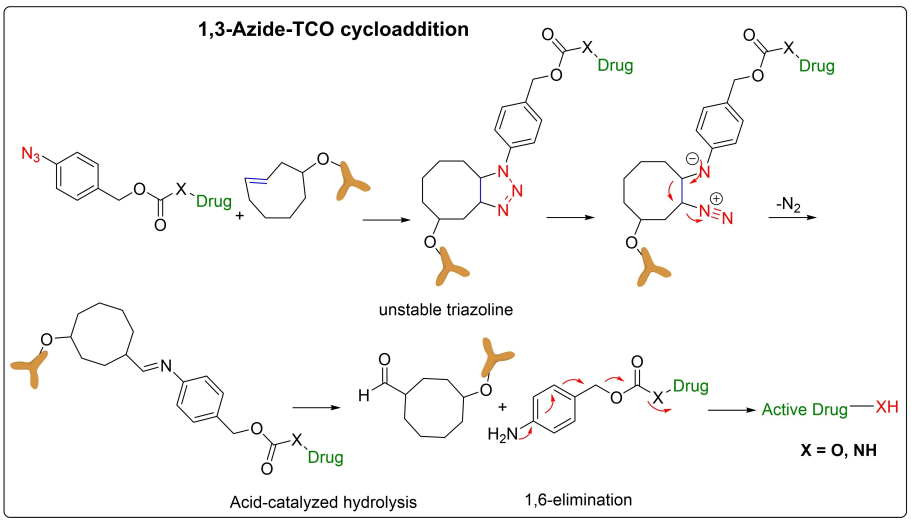

Figure 4. Cycloaddition of azide and *trans*-cyclooctene.

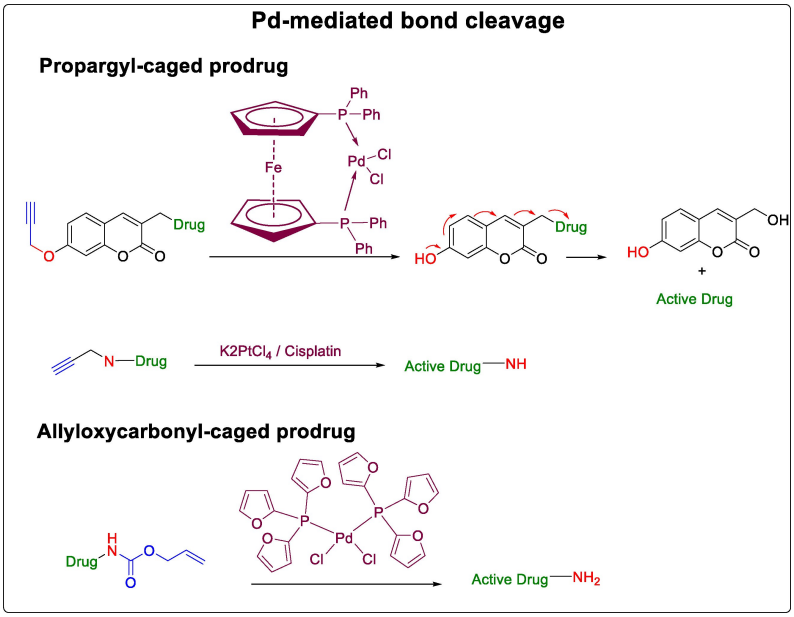

Figure 5. Palladium-mediated bond cleavage reactions.

complex encapsulated in a liposome to activate a nitrogen mustard prodrug linked to a coumarin fluorophore whose fluorescence was quenched by the intramolecular charge transfer effect of a propargyl group. The Pd complex catalyses a cascade starting with the depropargylation of the propargyl group to release the active drug moiety and release the quenching system which simultaneously activates the fluorophore.[92] Bernardes et al. reported the use of platinum-complexes (K_2PtCl_4 and cisplatin) for the decaging of pentynoyl tertiary amides and *N*-propargyls into secondary amines in the presence of water. Cisplatin-mediated depropargylation of a 5-flourouracil propargyl prodrug was also demonstrated in an *in vivo* zebrafish colorectal cancer model.[93]

2.6. Inverse electron demand Diels-Alder (IEDDA) reactions

IEDDA reactions involve a cycloaddition between a diene (i.e., tetrazine) and a dienophile with the elimination of N_2. The reaction was first reported in 2008 by Blackman et al.[94] and Devaraj et al.[95] Tetrazine has been reported to have [4+1] cycloadditions with isonitriles and [4+2] cycloadditions with *trans*-cyclooctenes.

2.6.1. [4+1] Cycloadditions of isonitrile with tetrazine

Tetrazines can react with isonitriles through either bioorthogonal ligation or cleavage. When primary and secondary isonitriles are used, isopyrazoles form and these isomerise to iminopyrazoles that eventually hydrolyse to form an aldehyde or ketone, and an amine, making them unsuitable for bioorthogonal ligation. Tertiary isonitriles are better suited for ligation reactions as the isopyrazoles thus formed are more stable; these do not isomerise and hence they only hydrolyse slowly in aqueous media[96] (Figure 6). The tertiary isonitrile-tetrazine reaction rate is high ($57.5\times10^{-2}\,M^{-1}s^{-1}$) and it has been reported to be used in metabolic glycan imaging *in vitro*.[97]

Tetrazine-isonitrile cycloadditions have also been reported to lead to bioorthogonal cleavage. [4+1] Cycloaddition reactions between 3-isocyanopropyl-masked probes and tetrazylmethyl derivatives proceed through cycloreversion, tautomerisation and hydrolysis under physiological conditions to release phenols and amines (Figure 6). In vitro, 3-isocyanopropyl-masked prodrugs of doxorubicin and mitomycin C were reported to be activated through reaction with a PEG-dipyridyl tetrazine activator to restore their potent drug activity in A549 adenocarcinoma cells.[98] In vivo, the same reaction was shown to restore the fluorescence of caged-dyes, and to release mexiletine after reaction of 3-isocyanopropyl-masked resorufin and tetrazylmethyl-caged-*O*-carboxymethyl fluorescein in zebrafish embryos.[99]

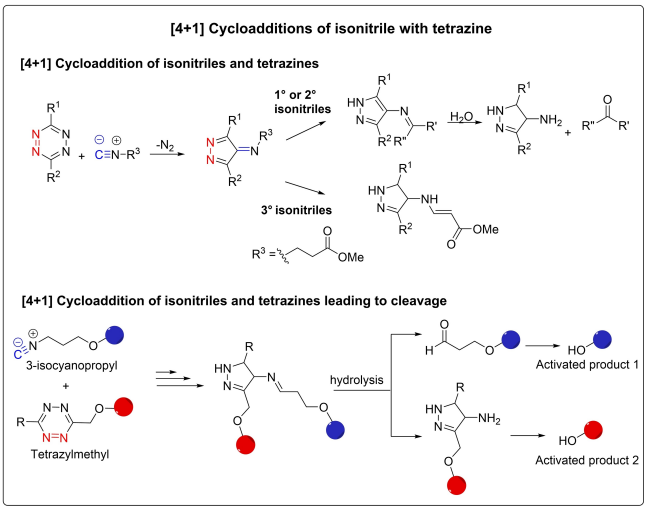

Figure 6. [4+1] Cycloaddition reactions of isonitriles and tetrazines.

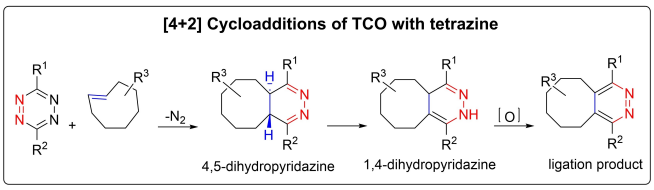

Figure 7. [4+2] Cycloaddition of *trans*-cyclooctene and tetrazines for ligations.

2.6.2. [4+2] Cycloadditions of trans-cyclooctenes with tetrazine

Strained alkenes such as TCO are the most common dienophiles used for tetrazine ligation. Thus 1,2,4,5-tetrazines react with TCO to form fused dihydropyridazines with very high reaction rates making the reaction very suitable for applications in biological systems[100] (Figure 7). Many dienophiles have been incorporated including bicyclononyne (BCN),[101] norbornenes,[95] cyclopropenes,[102,103] and *N*-acylazetine.[104] Vinylboronic acids (VBAs) were also introduced as stable, nontoxic and water-soluble non-strained dienophiles offering high reaction rates ($27\,M^{-1}s^{-1}$).[105] In terms of stability, TCO can isomerise to its less reactive *cis*-isomer in the presence of thiols.[106] Dioxolane-fused TCO (d-TCO) has been reported to be a more stable replacement affording a higher reaction rate.[107] The stability of tetrazines in aqueous environments is low when an electron withdrawing group is present at the 3 and 6 positions. Monomethyl tetrazines[108] and 1,2,4-triazines[109] have been reported to be more stable to hydrolysis. As tetrazine ligation by the IEDDA reaction is the fastest click bioorthogonal reaction ($k_2 = \sim 2000\,M^{-1}s^{-1}$) in biological systems, it is the most commonly used bioorthogonal reaction *in vivo*.

Robillard et al. have reported the functionalisation of TCO–Tz in order to establish bioorthogonal cleavages that be used for prodrug activation.[110] An axial carbamate-linked drug (e.g., doxorubicin) is attached at the allyl position of the TCO moiety and upon reaction with tetrazine, the 4,5-dihydropyridazine ligation product isomerises to a 1,4-dihydropyridazine which releases the carbamate-linked drug by decarboxylation (Figure 8). The reaction was proved to release the active doxorubicin *in vitro* with relatively fast kinetics. The reaction was further applied *in vitro* for protein activation,[111] and also *in vivo* for in-situ activation of prodrugs, imaging probes and enzymes in tumours. For example, a DOX-TCO prodrug has been selectively activated *in vivo* by an IEDDA in many approaches, one of which involved the separate encapsulation of DOX-TCO and the tetrazine derivative in micellar nanoparticles that were unstable at low pH and upon exposure to matrix metalloproteinase 2, These conditions therefore lead to site-specific prodrug activation.[112]

Another approach involved the usage of phosphatase enzyme-instructed supramolecular self-assembly systems to allow accumulation of tetrazine-bearing self-assembly precursors in cancer cells for selective activation of DOX-TCO in HeLa tumour-bearing mice.[113] Antibody drug conjugates (ADCs) have also been used to selectively deliver anti-TAG72 mAb CC49-tagged DOX-TCO for in situ activation by tetrazine-dextran activators in a colon cancer mice model.[114] TCO-linked monomethyl auristatin E (MMAE) has been reported to be formulated as an ADC through its linking of PEG to anti-TAG72 mAb CC49. Its in-situ activation by tetrazine-PEG activators in colon cancer and ovarian mice models was demonstrated.[115] Imaging probes such as the hemicyanine NIR dye have been caged by TCO for *in vivo* activation by carbon nanotubes bearing tetrazines, for tumour imaging in colon carcinoma-bearing mice.[116] Caging of the key lysine residue in the kinase ATP-binding pocket with TCO and using tetrazine to activate it

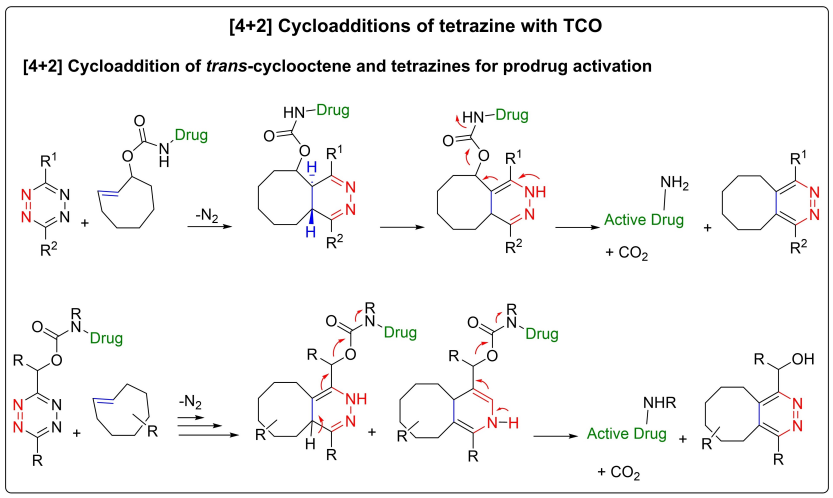

Figure 8. [4 + 2] Cycloaddition of *trans*-cyclooctene and tetrazines for prodrug activation.

has been reported for controlled and selective kinase activation. Luciferase's key lysine residue (K529) was masked with TCO, and HEK293T cells expressing the fLuc-K529TCOK variant were injected in mice before subsequent activation through an injection of dimethyl tetrazine.[117]

Recently, Robillard et al. reported a new mechanism for bioorthogonal cleavage involving TCO and tetrazine where the carbamate payload is installed on the tetrazine instead of the TCO. This modification boosts the reactivity of the TCO moiety increasing the reaction rate by three orders of magnitude compared to the parent TCO-tetrazine cleavage reaction, whilst also allowing simple non-allylic substituted TCOs to be used. The reaction was validated *in vitro* by using an ADC comprising a mAb CC49 with tetrazine-linked monomethyl auristatin E (MMAE), in-situ activation by TCO, and human colorectal cancer cells.[118]

A complementary cleavage system reported in 2016 by Devaraj et al. comprised a tetrazine and a vinyl ether-caged compound (active drug/dye). After a cascade ligation-elimination reaction, the tetrazine is converted into a diazine compound releasing the caged compound[119] (Figure 9). The reaction was further applied *in vivo* to activate a vinyl ether-masked camptothecin prodrug encapsulated in liposome using a tetrazine derivative either encapsulated in a separate liposome[120] or a PEGylated tetrazine on gold nanorods[121] for tumour chemotherapy and photothermal therapy.

In 2017, Bernardes et al. reported vinyl ether-tetrazine systems for the traceless release of alcohols in cells, with vinyl ether duocarmycin being successfully activated by a tetrazine derivative *in vitro*.[122] This concept was further developed by Bradley et al. to allow the traceless activation of two prodrugs simultaneously, where both tetrazine and vinyl ether were used as masking groups for two different drugs.[123]

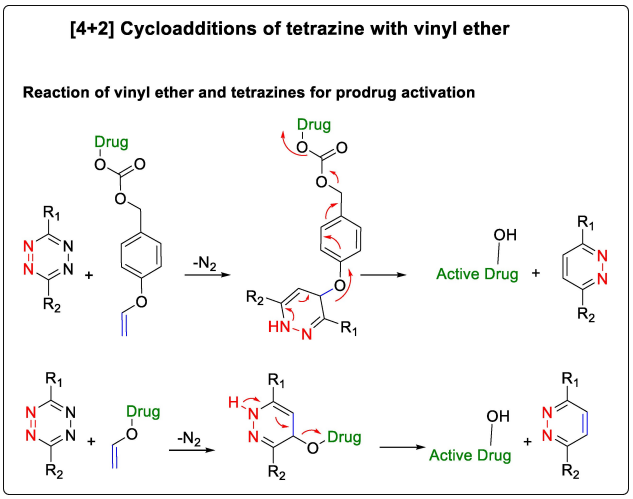

Figure 9. [4 + 2] Cycloaddition of vinyl ether and tetrazines for prodrug activation.

2.7. SuFEx click chemistry

Sulfur (VI) fluoride exchange (SuFEx), reported by Sharpless, involves the application of S(VI)-F motifs such as arylflourosulfates as connective linkers in polymer synthesis.[124,125] This pioneering work has promoted the development of covalent protein drugs through a latent, bioreactive, fluorosulfate-L-tyrosine (FSY) amino acid that is genetically encoded in a programmed cell death protein-1 (PD-1). This has been used *in vivo* in immunodeficient lung cancer and glioblastoma mice models (Figure 10). The covalently bonded, non-hydrolysable, linkage between PD-1 and PD-L1 results in an irreversible antagonist which restores the antitumour immune response.[126] SuFEx click chemistry also underpinned the more recently reported covalent nanobody-based PROTAC strategy for the targeted degradation of membrane proteins. Nanobody chimeras engineered with bioreactive amino acids including FSY are

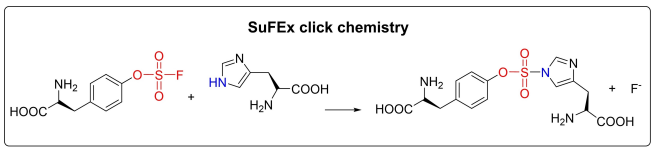

Figure 10. Sulfur (VI) fluoride exchange "SuFEx" click chemistry.

designed to irreversibly react with membrane proteins in order to trigger the internalisation and degradation of the protein.[127] Covalent protein mini-binders engineered with FYS have also been reported to irreversibly block the spike receptor binding domain in different SAR-COV-2 variants preventing their immune escape and providing a therapeutic strategy against SARS-CoV-2.[128]

3. Targeting Mechanisms

One of the most important factors that affects the success of bioorthogonal reactions' applications *in vivo* is the method used to deliver the bioorthogonal components. This section reviews the main targeting mechanisms (metabolic bioengineering, active targeting, passive targeting and simultaneously used strategies) that are reported for selective delivery of the bioorthogonal components to the desired site of action, as summarised in Figure 11.

3.1. Metabolic bioengineering

Metabolic bioengineering is the use of unnatural reporter-modified metabolic precursors to interfere with the normal biosynthetic pathways of biomolecules to finally express these unnatural reporters on cell surfaces. This concept has been used to intercept the biosynthesis of cell surface glycans and phospholipids using modified monosaccharide precursors or modified choline analogues, respectively (Figure 12). These monosaccharide precursors or choline analogues are chemically modified to have a bioorthogonal component (usually an azide group) which enables the incorporation (i.e., delivery) of this bioorthogonal component to the cells.

3.1.1. Metabolic glycoengineering (MGE)

Metabolic glycoengineering (MGE) is an extensively developed technique in which functionalities that are not naturally present within cell glycans or any other molecule *in vivo*, are expressed within the cell-surface glycans through the interception of the biosynthetic pathways of glycans using unnatural monosaccharide precursors[129–131] (Figure 12A). In the context of

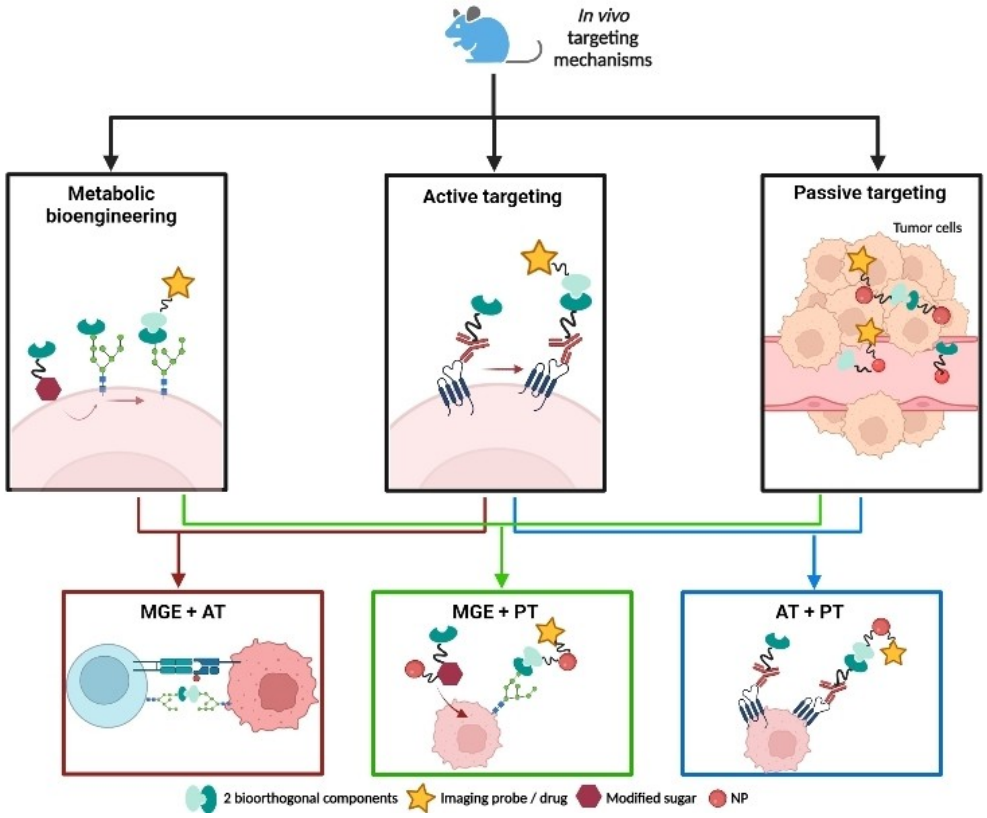

Figure 11. Summary of the main targeting mechanisms reported to deliver bioorthogonal components *in vivo*: Metabolic glycoengineering (MGE), active targeting (AT) and passive targeting (PT).

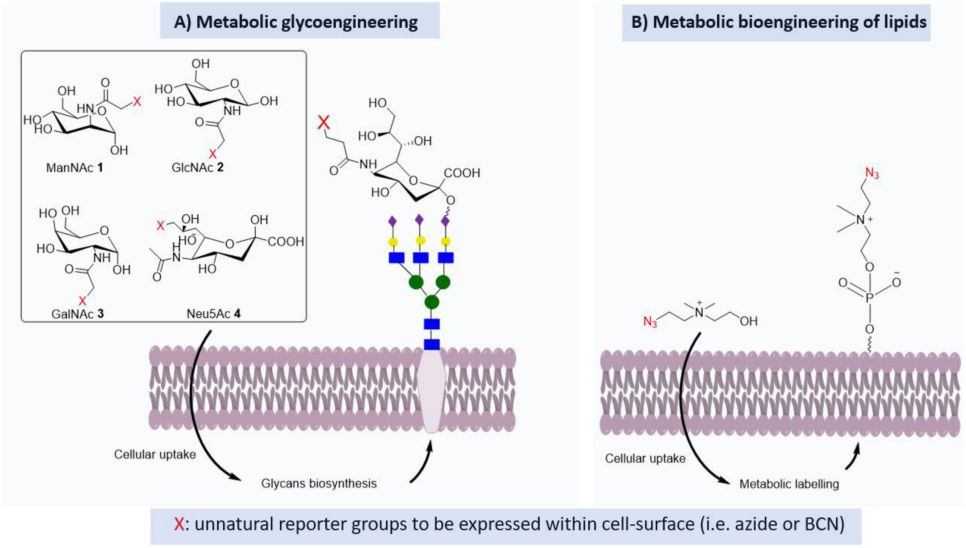

Figure 12. Metabolic bioengineering principle: A) Chemically modified monosaccharides that intercept the glycans' biosynthesis pathway and hence are expressed within cell-surface glycans. B) Azide-modified choline analogue that intercepts the phospholipids' biosynthesis pathway and hence expresses an azide within cell-surface phospholipids.

bioorthogonal reaction applications in biological systems, MGE provides a valuable means to deliver bioorthogonal components.

Many unnatural monosaccharides have been explored as substrates for MGE, among them: *N*-acetylmannosamine (ManNAc), *N*-acetylglucosamine (GlcNAc), *N*-acetylgalactosamine (GalNAc) and *N*-acetylneuraminic acid (Neu5Ac)[132–134] (Figure 12A). These substrates target the biosynthesis pathway for sialic acid. The most reported monosaccharide for MGE is *N*-acetylmannosamine (ManNAc), as it is the most efficient monosaccharide to intercept the biosynthesis of sialic acid leading to higher level of reporter group expression compared to GlcNAc and GalNAc. Once expressed on the cell surface, the reporter group can be chemically reacted with another moiety by click chemistry for delivery of dyes, imaging probes, radiolabelled probes, polymers and prodrugs.[49,135,136] Examples of the most used reporter groups (i.e., bioorthogonal components) that are delivered by MGE are azide[45] and bicyclo[6.1.0]nonyne (BCN).[73] The level of the reporter expression is dependent on the concentration of the modified sugar used for the MGE; the higher the concentration, the higher the level of incorporation and surface expression.

In vivo, the first bioorthogonal application that used MGE to deliver bioorthogonal components was labelling and tracking of therapeutic cells and biovesicles. Azide-modified monosaccharide precursors are used to engineer the azide bioorthogonal component on the cell surface glycans of these therapeutic cells. Then, the second bioorthogonal component (usually dibenzocyclooctyne DBCO or azadibenzocyclooctyne ADIBO) reacts with the azide reporter through click bioorthogonal chemistry. The DBCO/ADIBO component can be attached to a fluorescent dye, prodrug or targeting peptide for labelling and imaging, targeted drug release or enhanced targeting profile, respectively.[25,137–139]

Different types of therapeutic cells and biovesicles have been tracked *in vivo* by MGE and bioorthogonal chemistry to determine their fate and homing properties for degenerative diseases' therapies (Table 1). Although in many cases, cell labelling using bioorthogonal reactions is done *in vitro* first before the labelled therapeutic cell/ biovesicles is injected for *in*

Table 1. Summary of reported therapeutic cells and biovesicles that are metabolically glycoengineered to express an azide reporter, their bioorthogonal complementary probe and their reported *in vivo* model.

Therapeutic cells/biovesicles	Modified sugar for MGE	Complementary probe	Disease/ targeted tissue	*In vivo* model	Ref.
Human embryonic stem cells-derived endothelial progenitor cells "hEPCs"	Ac_4ManNAz Ac_4GalNAzAc_4GlcNAz	DBCO-CY5	Ischemic diseases	Hind limb ischemia mice model	[141]
Adipose tissue-derived mesenchymal stem cells "ADSCs"	Ac_4ManNAz	DBCO-RK, DBCO-ICG	Liver injury	Acetaminophen-induced acute liver failure model	[78]
Chondrocyte	Ac_4ManNAz	DBCO-650	Cartilage	Healthy mouse model	[77]
Exosomes	Ac_4ManNAz	DBCO-CY5	Lung adenocarcinoma	A549 tumour-bearing mice model	[76]

vivo tracking, the stability of the ligation bond is critical for optimum tracking results.

The advantages of the MGE technique are that it does not affect the proliferation ability of these cells, and it does not cause cytotoxicity either to the therapeutic cells or to the host cells. This makes the non-invasive MGE labelling technique safer compared to traditional fluorescence labelling agents that bind physically to therapeutic-cell membranes.[140]

In addition to labelling and tracking of cells and exosomes, the MGE approach has also been exploited in targeted prodrug activation for cancer therapy.[142] For this, MGE is used to deliver the activator part of the bioorthogonal reaction (azide), then the prodrug (cisplatin conjugated to DBCO) reacts with the azide groups on the cancer cells. Instead of using Ac_4ManNAz, histone deacetylase/cathepsin L-responsive acetylated azido-mannose (DCL-AAM) was used. As histone deacetylase (HDAC) and cathepsin L (CSTL) are overexpressed enzymes in tumour cells,[143,144] DCL-AAM can be cleaved in tumour cells to release the azide-modified sugar for selective MGE and azide expression on the tumour cells' surfaces.

3.1.2. Metabolic bioengineering of lipids

A further metabolic bioengineering approach instead intercepts the biosynthesis of phospholipids within cell surface membranes using an azide-modified choline analogue, azidoethylcholine (azide-Cho;[145] Figure 12B). The installed azide groups are then targeted by DBCO/ADIBO in a bioorthogonal reaction to deliver dyes. This strategy has been applied in labelling and *in vivo* tracking of exosomes that were separated from different tumours cells (MCF-7, MDA-MB-231 and HS578T) to determine the fate of each type.[145]

3.2. Active targeting

Active targeting utilises ligands such as antibodies,[146] peptides,[147] proteins[148] and small molecules such as folate[149] that selectively bind to their complementary antigens or receptors on cells for selective delivery. Ab–Ag selectivity makes active targeting advantageous in bioorthogonal components' selective delivery *in vivo* despite the weak interaction (compared to covalent binding), the limited number of specific Ab–Ag, and tumour heterogeneity.[150] It has been widely used for delivering drugs and theranostics to tumour cells.[151] This section will review how the active targeting principles are applied *in vivo* for bioorthogonal applications and the types of active targeting moieties that have been used.

3.2.1. Monoclonal antibodies (mAbs)

Monoclonal antibodies (mAbs) are the most reported active targeting moieties for *in vivo* applications of bioorthogonal reactions. They are functionalised in radioimaging and radiotherapy of tumours through their conjugation to radionuclides. However, these radiolabelled mAbs suffer from long half-lives and long circulation times which usually results in off-site accumulations. In addition, synthesis of some radiolabelled mAbs like cetuximab can be complex, for example requiring high temperatures and lengthy processes. Active targeting in conjugation with bioorthogonal reactions has aided in overcoming these limitations.[152]

Various antibodies have been used to target different tumour antigens (Table 2). The strategy requires conjugation of a bioorthogonal component (usually *trans*-cyclooctene TCO) with the mAb, the bioorthogonally tagged mAb then actively targets the tumour. This first step, termed pretargeting (discussed in Section 4), is essential to ensure the efficient

Table 2. Summary of reported mAbs/peptides that are conjugated to bioorthogonal moieties, their antigen/receptor, their bioorthogonal complementary probe and their reported *in vivo* model.

Antibody/peptide	Antigen/ receptor	Complementary probe	Tumour	*In vivo* model	Ref.
Cetuximab-TCO	EGFR	^{68}Ga-Tz	Colorectal and head & neck cancers	EGFR-expressing A431 xenograft-bearing mice.	[158]
Cetuximab-d-TCO	EGFR	N_3-DOX prodrug	Melanoma	B16-F10-Luc2-EGFR cells-bearing mice	[83]
CC49-TCO	TAG-72	^{99m}Tc-Tz	Pancreatic and colon cancers	LS174T colon cancer-bearing mice	[159]
CC49-TCO-DOX	TAG-72	^{177}Lu-Dextran-Tz	Pancreatic and colon cancers	LS174T colon cancer-bearing mice	[114]
CC49-TCO-MMAE	TAG-72	^{111}In-PEG-Tz	Pancreatic and colon cancers -Ovarian cancer	LS174T colon cancer-bearing mice -OVCAR-3 xenograft-bearing mice	[115]
THIO-MAB-TCO	HER2	^{111}In-Tz	Breast and gastric cancers	HER2$^+$ mouse model	[153]
huA33-TCO	A33	^{64}Cu-Tz	Colorectal cancer	A33 antigen-expressing SW1222 colorectal cancer-bearing mice	[160,161]
Anti-CEA 35 A7-TCO	CEA	^{177}Lu-Tz	Peritoneal carcinomatosis	Orthotopic tumours (A431-CEA-Luc cells)-bearing mice	[162,163]
Anti-TSPAN8-TCO	TSPAN8	CY5-Tz	Peritoneal carcinomatosis	Human HT29 xenograft- bearing mice	[163]
Anti-PSMA-TCO	PSMA	MB-Tz	Prostate cancer	Prostate carcinoma-bearing mice	[164]
GEBP11 vascular-homing protein-TCO	GEBP11 receptor	CY5.5-Tz	Gastric tumours	Human gastric carcinoma xenograft-bearing mice	[157]
Dimeric NGR-DBCO	CD13 receptor	CY5.5-N_3	Prostate, colon and pancreatic cancers	HT-1080 tumour-bearing mice	[79]

arrival of the first bioorthogonal component to the targeted site of action by active targeting. The second step is the conjugation of the second bioorthogonal component (usually tetrazine Tz) with the radionuclide/fluorescent dye that will be selectively delivered to the tumour site through the bioorthogonal reaction between TCO and Tz (Figure 13A).

This strategy has been applied *in vivo* in different imaging techniques (positron emission tomography (PET), single-photon emission computerised tomography (SPECT) and ultrasound imaging) and radioimmunotherapy of tumours. The efficiency of this strategy is dependent on many factors, first is the level of antigen expression on the targeted tumours. High levels of antigen expression are required to ensure significant accumulation of the first bioorthogonal component at the tumour site. However, targets in solid tumours are only overexpressed in a limited number of cancer patients making the attainment of sufficient accumulation *in vivo* very challenging. Second is the influence of the bioorthogonal modification on the antibody's immunogenicity and pharmacokinetics. TCO modification is reported to not generally affect an antibody's immunogenicity, but in a few cases such as for the THIO-MAB antibody, it influenced its pharmacokinetics by increasing the antibody serum half-life leading to high blood radioactivity after the administration of the Tz-tagged radionuclide.[153] Third is the characteristics of the radionuclide used. Radionuclides with a short half-life (i.e., ^{68}Ga) might have limited usage even with the pretargeting strategy due to their rapid clearance. Radionuclides with hydrophobic characteristics (i.e., ^{99m}Tc) also cause high background distribution.

In the context of optimising the bioorthogonal reactivity and pharmacokinetics of the two components, PEGylation has been widely used. A PEG linker is added either between the TCO moiety and the Ab (increasing the TCO group's loading on the Ab and thus increasing reactivity with Tz radionuclides) or between the Tz and the radionuclide. With Anti-CEA 35 A7 mAb[154] and anti-TSPAN8 mAb (Ts29.2),[155] the PEGylation of Abs increased the average number of TCO moieties conjugated to the Abs especially when increasing the PEG chain length ($n=12$), but it inversely affected the efficiency of the click reaction between TCO and Tz. The PEG linker between the Tz moiety and the radionuclide is hypothesised to improve the radioligand's pharmacokinetic parameters. However, a long PEG chain length ($n=11$) increased the radionuclide clearance due to its higher hydrophilicity. These studies suggest that the PEGylation of the radiolabelled-Tz probe is more functional than PEGylation of the TCO-modified antibody and can add to the selectivity that is established by active targeting and bioorthogonal reaction.

Using antibodies for targeted delivery of the TCO moiety has also been implemented for prodrug activation in situ through bioorthogonal reactions (TCO with Tz or azide). In pancreatic and colon cancers, a TCO-DOX/MMAE prodrug is attached to the CC49 mAb and injected first for pretargeting, then the complementary Tz is injected for prodrug activation.[114,115] For melanoma, cetuximab-TCO is injected first for pretargeting, then the azide-DOX prodrug is injected for activation.[83] As TCO is known for its instability in blood, due to its isomerisation into the unreactive *cis*-isomer upon contact

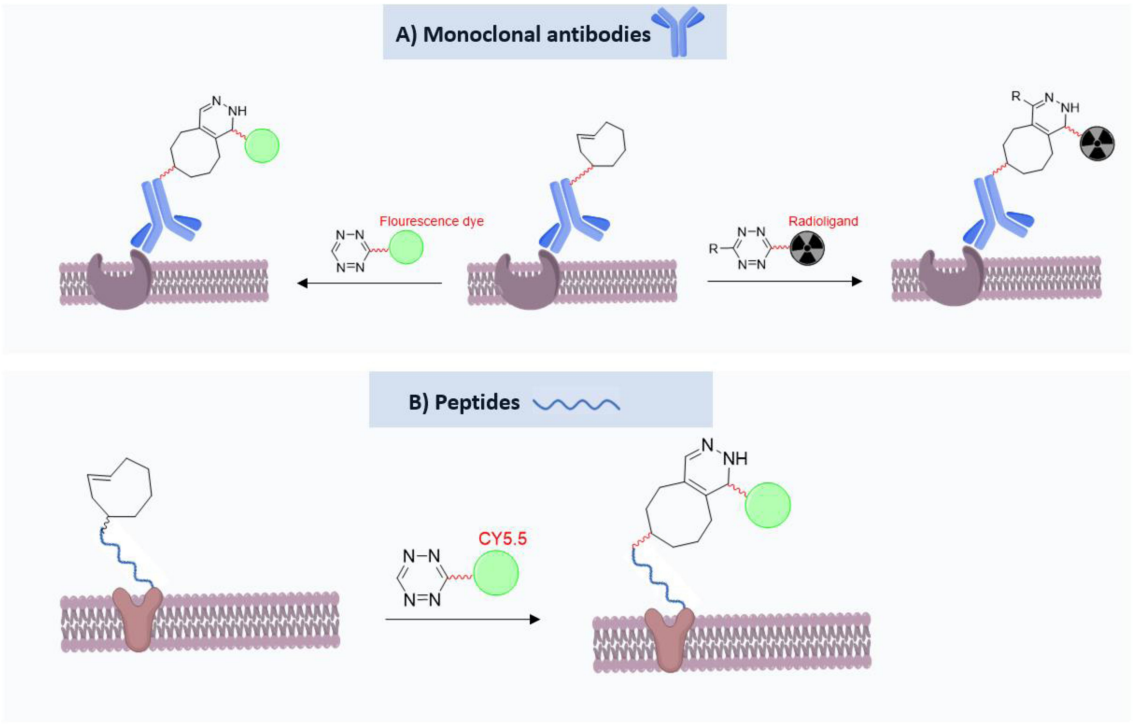

Figure 13. Active targeting: A) Tumour-targeting by TCO-modified mAbs followed by radiolabelled/fluorescence Tz. B) Tumour-targeting by TCO-modified peptides followed by fluorescence Tz.

with serum proteins and albumin,[156] many strategies have been tested to minimise this deactivation. One strategy introduced rigidity through a *cis*-dioxolane-fused TCO (cetuximab-d-TCO), resulting in decreased TCO isomerisation alongside a four- to six-fold increased rate of activation. These advantages are notable and to a certain extent compensate for the lower physiological stability ($t_{1/2}$ ~ 24 h in 50% serum) of the modified TCO compared with simpler TCO forms ($t_{1/2}$ ~ 5 days).[83] Inserting a spacer such as a lysine-branched spacer with a PEG_{24} moiety between the TCO and the mAb also proved valuable for shielding the TCO from interaction with copper-binding sites in serum proteins and hence minimised its subsequent isomerisation ($t_{1/2}$ ~ 24 h in 50% mouse serum).[115]

3.2.2. Peptides

Some studies have used peptides as the active targeting moiety (Table 2). While in both cases this strategy has been applied for fluorescence imaging of tumours, in principle the same strategy can be applied for the delivery of drugs. As discussed for mAbs, the peptides are conjugated to one bioorthogonal component (TCO for the IEDDA reaction[157] or DBCO for the SPAAC reaction[79]) while the fluorescent dye (CY5.5) is conjugated to the second bioorthogonal component (Tz for the IEDDA reaction or azide for the SPAAC reaction). The bioorthogonal approach improved the tumour accumulation and fluorescence imaging compared to direct labelling of peptides with dyes (Figure 13B).

3.2.3. Challenges in the use of active targeting

Antibody-based therapeutics have achieved fast growing success, with more than 70 antibody-based therapeutics already in clinical use. However, many challenges should be considered when suggesting antibodies for targeting purposes. These include the heterogeneous nature of the targets on cancers cells, interactions with the host immune system, the tissue's accessibility and more general pharmacokinetic considerations like blood circulation time and clearance. Moreover, since the antibodies targets are often expressed, albeit at lower levels, on normal cells, off-site interactions are also likely to occur.

The level of radiolabelling achieved by active targeting mechanisms *in vivo* for bioorthogonal applications has been reported to be promising (in terms of magnitude and time). The pretargeting strategy (further discussed in Section 4) has also improved the labelling practice by lowering the doses needed for *in vivo* labelling. TCO-mAb doses required for labelling *in vivo* are reported to be around 100 μg (or around 0.7 nmol) which are reported to be sufficient for subsequent labelling by radionuclides (ca. 10 MBq or 0.7 nmol) over 24–48 h.[153,159–161] Translation from *in vivo* to clinical settings needs careful consideration particularly for parameters such as the binding rate between the mAb and its target, the radionuclide dose, and the labelling time. In terms of the radionuclide dose, the dilution factor increases when transferring from *in vivo* to clinical setting, this may lead to a decrease in the concentration of the bioorthogonal reaction component which may impair the reaction rate and efficiency. In terms of binding rate, for mAbs with high binding rates, the association k_{on} and dissociation k_{off} between the mAb and target are affected by the mAb diffusion rate which means they will depend on the tumour environment rather than the binding rate. mAbs with high affinities k_D (pM or nM) require a long time (hours to days) to reach binding equilibrium with their targets.[165,166] Therefore, even with high affinity Abs, long labelling times are required which make translation of the prelabelling approach to the clinic very challenging.

3.3. Passive targeting

Passive targeting is a targeting mechanism in which drugs or drug delivery vehicles reach their targeted delivery site as a result of their physicochemical properties such as size or lipophilicity. Many *in vivo* applications for bioorthogonal reactions have used nanoparticles for the targeted delivery of one or both the bioorthogonal components.

3.3.1. Enhanced permeability and retention (EPR) effect

The vast majority of studies that have suggested passive targeting mechanisms for the delivery of bioorthogonal components rely on the enhanced permeability and retention (EPR) effect. This concept has been mainly applied for cancer-related applications because in tumours, the leaky neovasculature allows the passive accumulation of molecules with certain size (10–500 nm; > 40 KDa).[167–169] For drugs and probes to be delivered by this passive mechanism, they are typically required to circulate for an appropriate time to allow accumulation. Therefore, one of the mechanisms to deliver the bioorthogonal components selectively to tumour sites is their conjugation with a nanovehicle to increase their circulation time.

Tumour accumulation of bioorthogonal components by the EPR effect can be quantified according to the level of radioactivity, in imaging applications, and by fluorescence intensity, in prodrug activation applications. The level of tumour accumulation (i.e., tumour-to-tissue ratio) that was observed was very heterogenous and ranged from one-fold and less[170,171] to eleven-fold.[120,121,172–174] This variation is highly affected by the clearance rate of the nanoparticles from the body.

Some studies hypothesise passive accumulation through the EPR effect, but do not measure the actual extent of it. For instance, some systems designed to accumulate into tumours through the EPR effect, are, in fact, directly injected intratumourally during *in vivo* testing.[58,92]

While an extensive discussion of the EPR effect is beyond the purpose of this review, it should be noted that the EPR effect is much more complex and variable than originally thought.[175,176] For example, some have argued that the EPR effect is essentially a murine artefact.[175,177] Others have proposed that different transport mechanisms underpin macro-

molecular accumulation in tumours.[169,178] Perhaps the most interesting research in this field has shown remarkable heterogeneity in the magnitude of the EPR effect across different patients, which has also been shown to be affected by tumour characteristics like type and stage. Additional strategies have been suggested to maximise the EPR effect (and perhaps even bypass the need for it altogether). Techniques known to affect tissue permeability like radiotherapy and hyperthermia have been proposed by inducing endothelial cell apoptosis.[179,180] Antiangiogenic drugs,[181] inflammatory cytokines and vasodilators[182] are suggested to modify tumour blood flow and vascular permeability. Functionalising nanoparticles to incorporate tumour-targeting moieties to bind selectively to complementary moieties in tumours (i.e., combining active and passive targeting principles to achieve more selective tumour retention) is another valued approach.[183,184] As such, in relation to bioorthogonal reactions, studies reporting delivery of one or more of the components through the EPR effect should be considered with caution, in this quickly developing context.

3.3.2. Passive targeting of the bioorthogonal components

In the context of passive targeting, one or both components of the bioorthogonal reaction, could be delivered by passive targeting.

Application to one component: Some studies have applied the passive targeting concept to deliver only one component of the bioorthogonal reaction. These studies are mainly *in vivo* imaging applications, either tumour imaging[170–172] or atherosclerosis imaging.[173] One bioorthogonal component is solely delivered by passive targeting (usually the TCO moiety) while the second bioorthogonal component (Tz) is conjugated with the radiolabelled nuclide purposed for imaging and delivered systemically (Figure 14A).

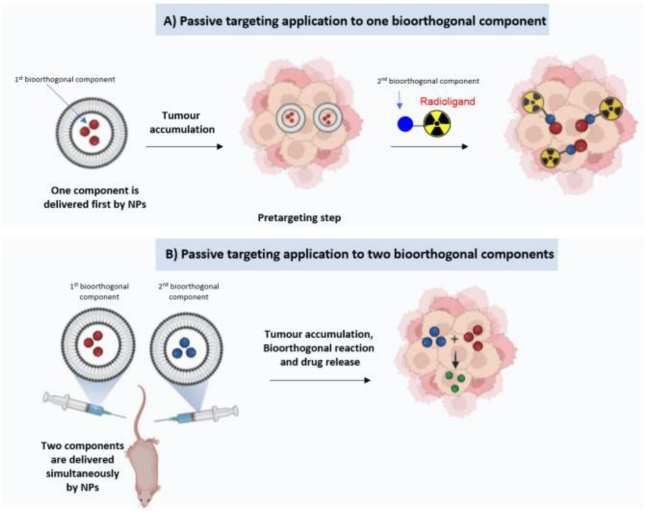

Figure 14. Passive targeting. A) Delivering one bioorthogonal component only by passive targeting. B) Delivering both bioorthogonal components by passive targeting.

Application to both components: Conventional bioorthogonal-based prodrug activation requires stepwise administration of the prodrug and trigger in order to avoid early activation. This stepwise administration is difficult to optimise to afford the desired ratio of both components at the desired site of action and needs extensive metabolism studies which makes its clinical application more challenging. Using nanoparticles provides a means to solve this problem as it enables the encapsulation of each component (prodrug and trigger) in a separate nanoparticle for co-administration. Both nanoparticles can effectively reach the tumour site without premature contact between the prodrug and the trigger (Figure 14B).

This has been proposed for the delivery of anti-cancer drugs such as camptothecin (CPT),[120,121] nitrogen mustard,[92] combretastatin A4[174] and nitrogen oxide (NO).[185] They are first converted to prodrugs and encapsulated into a phospholipid liposome and the trigger is encapsulated in a separate phospholipid liposome[92,120] or immobilised on a nanorod.[121] With combretastatin A4, two analogues of the drug precursors (i.e., azide and alkyne analogues) are encapsulated in a nanocapsule and the bioorthogonal catalyst (i.e., copper nanocatalyst) is encapsulated in a different nanocapsule. At the tumour site, the catalyst commences the bioorthogonal reaction between the two precursors for in-situ drug synthesis.

Other than prodrug activation, the same strategy can be applied to other *in vivo* bioorthogonal applications including tumour imaging. Each of the bioorthogonal components is enclosed in a separate nanoparticle and one of them can be modified with a radiolabelled nuclide for imaging.[58]

3.3.3. Types of nanosystems

The nanocarriers for the bioorthogonal components vary between organic-based nanoparticles (i.e., liposomes) and inorganic-based nanoparticles (i.e., gold nanorods) according to the application purpose. Variations in the type and size of the used nanoparticles (Table 3) affect the tumour accumulation rate, which ranges from five minutes[170] to hours[120,121,171] and days.[172–174,185] Nanoparticles with smaller sizes like nanostars and mesoporous silica nanoparticles have the slowest tumour accumulation rates (3 and 6 days, respectively).

In addition to variations in the size and type of the nanosystems used to deliver the bioorthogonal components, the nature of conjugation between the nanoparticle and the bioorthogonal moiety that it is carrying also varies. This conjugation is either physical or chemical. For example, chemical modification of the nanoparticle surface can allow incorporation of the bioorthogonal moiety that is to be delivered. Usually a PEG polymer linker is inserted between the surface functional groups (i.e., amino or thiol group) on the nanoparticle surface and the bioorthogonal moiety[121,172,173] rather than direct chemical attachment[170] for better biocompatibility (i.e., decreasing captivation by spleen, liver and lungs and increasing blood circulation time).[186] Physical conjugation involves encapsulation of the bioorthogonal moiety inside the nanoparticle. Nanoparticles with smaller sizes like nanostars,

Table 3. Summary of reported nanoparticle vehicles that are used to deliver bioorthogonal moieties, their sizes, their bioorthogonal complementary probe and their reported *in vivo* model.

Nano particle	Size	Complementary probe	Tumour	*In vivo* model	Ref.
Supramolecular nanoparticles-TCO	100 nm	^{64}Cu-Tz	Solid tumours	U87 glioblastoma -bearing mice.	[171]
Nanostars-TCO	13, 14 and 40 nm	^{18}F-Tz	Solid tumours	CT26 colon cancer-bearing mice.	[172]
Mesoporous silica nanoparticles-TCO	N/A	^{11}C-Tz	Lung	Healthy mouse.	[170]
Mesoporous silica nanoparticles-DBCO	60–80 nm	^{18}F-N_3	Subcutaneous tumours and atherosclerosis	Subcutaneous U87MG tumour-bearing mice and ApoE − /- mice (atherosclerosis) mice.	[173]
Liposome-Oa	136 nm	^{64}Cu-Ald	Breast cancer	4T1 tumour-bearing mice.	[58]
Liposome-CPT-vinylether	105-200 nm	Liposome-dye-Tz	Metastatic cervical cancer	HeLa tumour-bearing mice	[92,120,121]
Liposome-N mustard- propargyl		Liposome- Pd-DPPF			
cLANC-azide and alkyne analogues of combretastatin A4 precursors	N/A	cLANC-Cu	Colorectal cancer	HT29 tumour-bearing mice.	[174]
Liposome-NO donor	71, 131 nm	Liposome-Tz	Melanoma, glioma and colon cancer	HCT-116 cells implanted into the yolk sac zebrafish embryos	[185]
Tz-Single-walled carbon nanotubes	200 nm long	TCO-hemicyanine	colon cancer	CT26 tumour-bearing mice	[116]
Tz-hydrogel	12 nm	TCO-Doxorubicin	Metastatic cervical cancer	HeLa tumour-bearing mice	[113]

nanorods and mesoporous silica nanoparticles are usually chemically conjugated with the bioorthogonal moiety, while larger nanoparticles like supramolecular nanoparticles, liposomes and cross-linked lipoic acid nanocapsule physically encapsulate the bioorthogonal moiety.

Recently, the Shasqi company reported the development of a CAPAC™ (click activated protodrugs against cancer) platform, which is currently under phase 1/2a clinical studies (ClinicalTrials.gov Identifier: NCT04106492). A click reagent (tetrazine-modified sodium hyaluronate-based biopolymer) is injected locally in the tumour to subsequently activate a systemically infused protodrug (TCO-modified cytotoxic doxorubicin). In vivo, the maximum tolerated dose (MTD) of the combined SQL70 (Tz-biopolymer) and SQP33 (TCO-doxorubicin) was found to be 19.1 times higher than the conventional doxorubicin. Moreover, a single-dose injection of SQL70 was able to activate multiple SQP33 doses (10.8 times the MTD of doxorubicin) as it retains its activity over a 5-day dosing period.[187,188]

3.4. Simultaneously used strategies

Combining two or more of the previously discussed targeting strategies (i.e., MGE, active and passive targeting) has been proposed with the aim of enhancing their advantages, and addressing the challenges of each individual strategy.

3.4.1. MGE with passive targeting

Passive targeting has been combined with MGE for applications of bioorthogonal reactions in three approaches. The first approach used nanoparticles to passively deliver a modified sugar intended for MGE (first component of the bioorthogonal reaction). The second approach used the nanoparticles to passively deliver the imaging probe/drug (second component of the bioorthogonal reaction). Finally, the third approach used nanoparticles to passively deliver both components (Table 4, Figure 15).

Passive delivery of the modified sugar: This approach has proved particularly valuable for targeting tumours and brain sialo-glycoproteins due to the physicochemical properties of

Table 4. Summary of azide-modified monosaccharides used for MGE, their bioorthogonal complementary probe, their nanovehicle and their reported *in vivo* model.

First component	Second component	Tumour	*In vivo* model	Ref.
Nano-MPs	ADIBO-CY5.5	Various tumours	U87 tumour-bearing mice	[190]
LIP-9-azido sialic acid	DBCO-650	Brain	Healthy mouse model	[191]
Ac_4ManNAz	Nano-BCN-CY5.5	Lung, brain and breast cancers	U87 tumour-bearing mice	[193]
Ac_4ManNAz	Nano-DBCO-DOX/ZnPc	Breast cancer	MCF-7 cells tumour-bearing mice	[194]
Ac_4ManNAz	Nano- triarylphosphine-Dox	Colorectal cancer	CT26 subcutaneous tumour-bearing mice	[47]
Ac_4ManNAz	Nano-BCN-CY5.5	Brain stroke	Healthy mouse and photothrombotic stroke mouse.	[195,196]
Nano- Ac_4ManNAz	LIP-DBCO-ZnPc	Solid tumours	A549 tumour-bearing mice	[197]

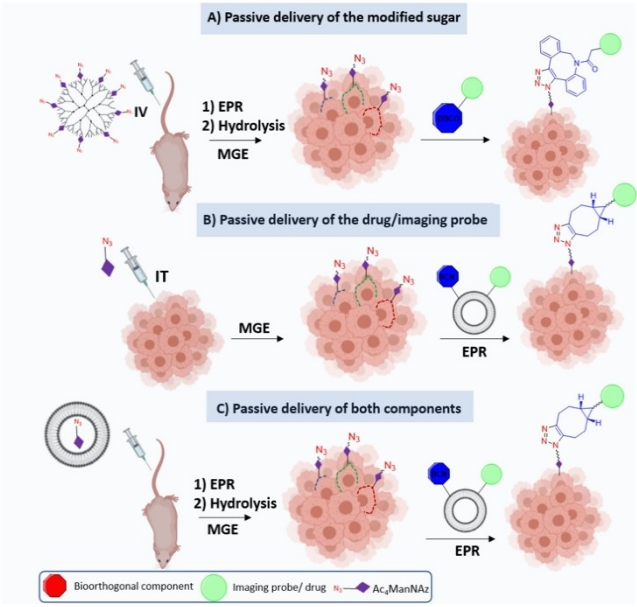

Figure 15. Combining MGE with passive targeting. A) Delivering only modified sugar by passive targeting. B) Delivering only imaging probe/drug by passive delivery. C) Delivering both components by passive targeting.

nanoparticles which enhance the delivery of the modified sugar.

In tumours, the EPR effect,[189] previously discussed, enhances the selective delivery of the modified sugar to tumour sites (Figure 15A). In this context, nanosized metabolic precursors (nano-MPs) which are composed of an Ac_3ManNAz-conjugated succinic acid-terminated generation-4 poly(amidoamine) dendrimer have been reported. These nano-MPs can localise in tumours more effectively than free metabolic precursors thus generating the azide reporters on tumour cells' surfaces specifically after the intravenous administration (4.7-fold higher than the free Ac_3ManNAz).[190]

For delivery to the brain, the lipophilic nature of liposomes has proved valuable for enhancing the ability of the modified sugars to cross the blood-brain barrier. A liposome-assisted bioorthogonal reporter (LABOR) approach has been developed in which the azide-modified sugars (i.e., 9-azido sialic acid and ManNAz) are encapsulated in liposomes to enhance crossing of the blood-brain-barrier.[191] Additionally, the liposomes were surface PEGylated for stabilisation and to extend their half-lives. Despite the efficient labelling of the brain sialoglycoproteins with the azide reporters (detected by fluorescent imaging after administration of DBCO-CY5), the lipophilic nature of the liposomes caused non-specific labelling in other organs as well. These results can be compared to the results from another strategy called "the piggybacking" strategy in which neuroactive carriers (valproic acid, nicotinic acid and theophylline-7-acetic acid) were used to deliver azide-modified sugars to brain cells for MGE[192] (Figure 16). In terms of selectivity, both strategies resulted in MGE and azide-reporter expression in other organs along with the brain. Hence, the combined approach did not solve the selectivity problem which makes the two strategies (i.e., piggybacking and LABOR) nearly equal in terms of benefits and drawbacks. These strategies could be beneficial in exploring the biofunctions of brain sialoglycans and understanding the development of neurological disorders but not for other purposes like selective drug delivery to brain.

Passive delivery of the imaging probe/drug: This approach makes use of the passive targeting concept for site specific delivery of the second bioorthogonal component conjugated to the imaging probe/drug after the MGE step takes place (Figure 15B). The limitation of this approach is that the azide-modified sugar (Ac_4ManNAz) has to be administered intratumourly to ensure site-specific MGE before the administration of the second bioorthogonal component. This approach has been used for *in vivo* fluorescence imaging of lung, brain and breast cancers[193] and for delivery of doxorubicin.[47,194] Another *in vivo* application for this approach is the labelling and tracking of stem cells. MGE of stem cells' surface glycans by Ac_4ManNAz is achieved first for azide expression, followed by their bioorthogonal reaction with BCN-modified nanoparticles which encapsulate different imaging agents.[195,196] Then, these labelled stem cells are administered *in vivo* for live tracking. This strategy does not involve intratumoural administration of any component. However, in terms of direct labelling of stem cells for *in*

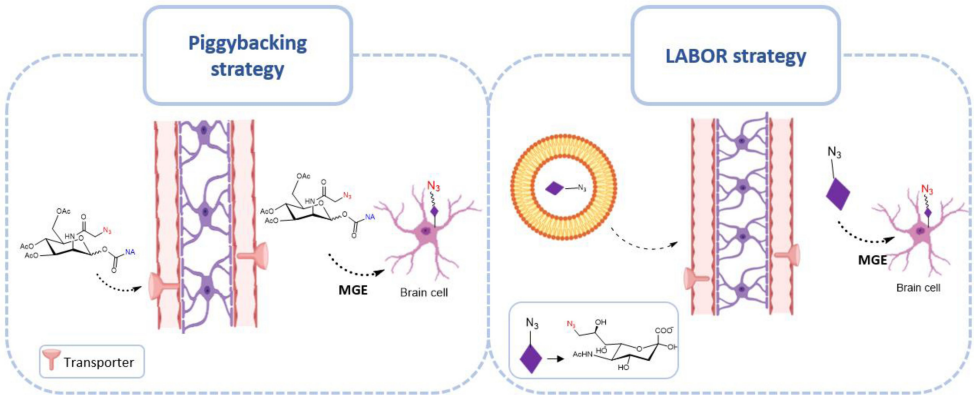

Figure 16. Illustration of the difference between the piggybacking strategy and LABOR strategy in labelling brain cells' surfaces.

vivo tracking, using the MGE alone as discussed in section 3.1.1. is much simpler in application and achieves the same purpose.

Passive delivery of both components: This approach makes use of the passive targeting concept for site specific delivery of both bioorthogonal components (Figure 15C). It has been particularly reported for *in vivo* photothermal therapy of solid tumours.[197] The azide-modified sugar (Ac_4ManNAz) and the photothermal probe zinc(II)-phthalocyanine (ZnPc) are loaded into nanocarriers (nanomicelle and liposome, respectively) for site-specific MGE in tumour cells followed by bioorthogonal reaction and generation of cytotoxic heat.

3.4.2. MGE with active targeting

Active targeting has been combined with MGE for studying T-cell therapy in solid tumours. Two strategies have been reported, both relying on the active recognition of T-cells by tumour cells. The first strategy focused mainly on labelling and *in vivo* tracking. MGE of T-cells' surface glycans by Ac_4ManNAz is first achieved for azide expression, followed by their bioorthogonal reaction with DBCO-CY5.5[198] (Figure 17A). This strategy allows tracking of T-cells' biodistribution and correlation with the therapeutic response observed. The second strategy focused on enhancing T-cells' therapeutic recognition *in vivo*. MGE of T-cells' surface glycans by Ac_4GalNAZ allows azide expression as well as MGE of tumour cells' surface glycans by Ac_4ManNBCN for BCN expression. Bioorthogonal reaction between azide and BCN, as well as antigen–antibody recognition of T-cells to tumour cells, enhances the recognition and thereby the immunotherapy effect[199] (Figure 17B).

3.4.3. Active targeting with passive targeting

Active targeting has been combined with passive targeting for the delivery of drugs and imaging agents in cancer and atherosclerosis *in vivo* (Table 5). The strategy suggests attaching one bioorthogonal component (usually *trans*-cyclooctene TCO) to a mAb to selectively bind to its antigen at the desired site of action. This is then targeted with Tz-modified nanoparticles (i.e., the second bioorthogonal component) which encapsulate

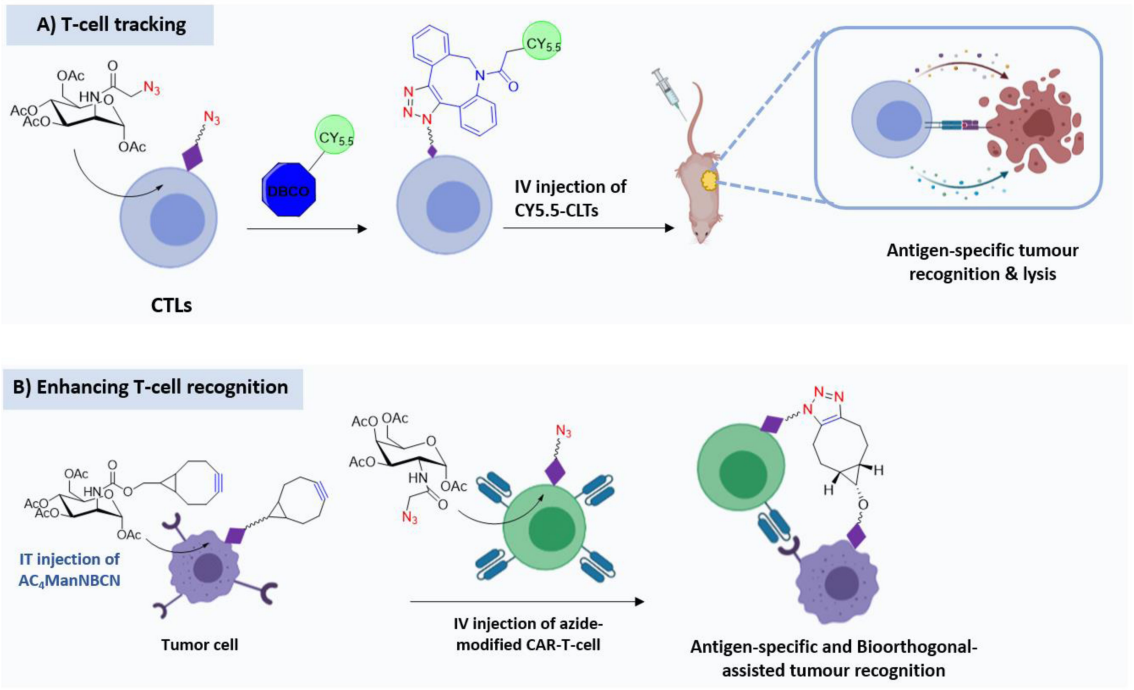

Figure 17. Combining MGE with active targeting. A) Labelling T-cells by MGE to track their therapeutic response. B) Enhancing T-cells' tumour recognition through MGE and bioorthogonal reaction.

Table 5. Summary of reported antibodies and nanoparticles that are conjugated to bioorthogonal moieties, their complementary antigens and their reported *in vivo* model.

First component	Second component	Antigen	Tumour	*In vivo* model	Ref.
CD11b-TCO	Dox-loaded MSNs-Tz	$CD11b^+$	Breast cancer	Orthotopic 4T1 breast tumour-bearing mice.	[200]
E-06-TCO	Tz-modified ^{68}Ga iron oxiDe nano-radiomaterial	Oxidised LDL and HDL	Atherosclerosis	Atherosclerosis mice model.	[201]

the imaging probe/drug (Figure 18). In tumours, combining both delivery techniques with the bioorthogonal chemistry ensured the deep delivery of the drug-loaded nanoparticles (i.e., doxorubicin-loaded mesoporous silica nanoparticles) into the avascular regions of the tumour instead of relying on the EPR effect alone to deliver the drug (two-fold higher).[200] In atherosclerosis, this strategy caused more selective accumulation of nano-radiomaterial in atherosclerotic plaques (five-fold higher).[201]

Another approach in combining active with passive targeting principles has been applied in the cell-based therapy of arterial wall injury.[202] Nanoparticles bearing glycoprotein 1bα (Gp 1bα) proteins and Tz are designed to target the injured endothelial surface through the interactions between Gp 1bα and von Willebrand factor (vWF) and hence coat the injured vasculature wall. Then, transplanted endothelium cells conjugated with TCO are delivered for rapid capture by Tz leading to homing of endothelial cells at the injury place.

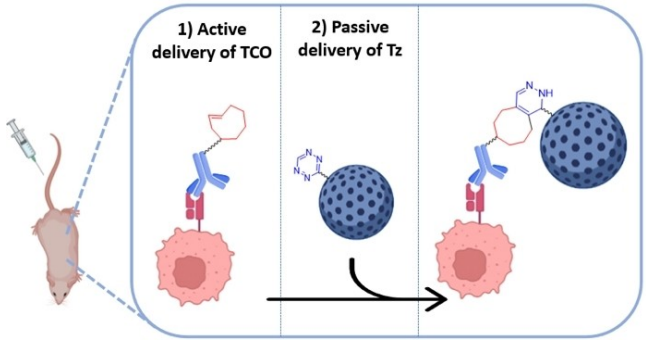

Figure 18. Combining active and passive targeting. Active delivery of TCO bioorthogonal component followed by passive delivery of the Tz bioorthogonal component in tumours.

3.4.4. MGE with active and passive targeting

When active targeting principles are applied together with other targeting mechanisms, the intention is usually to enhance the selectivity achieved by the bioorthogonal reaction. This is in contrast to when passive targeting is applied together with other targeting mechanisms, where the focus is to increase tumour accumulation. One study applied the three targeting mechanisms together to benefit from the enhanced recognition afforded by active targeting, and high tumour accumulation resulting from passive targeting, along with the high expression levels of bioorthogonal components achieved by MGE. This study enhanced photothermal therapy in breast, lung and hepatic tumours.[203] MGE was utilised to deliver both components of the bioorthogonal reaction, MGE of T-cells' surface glycans by Ac_4GalNAZ allows azide expression, and MGE of tumour cells' surface glycans by Ac_4ManNBCN facilitates BCN expression. Then, extraction of the T-cells' membrane which is labelled by azide is performed to coat a nano-photosensitiser (indocyanine green, ICG) to yield an azide-labelled T cell membrane-coated ICG-PLGA nanoparticle. The bioorthogonal reaction (azide-BCN) along with immune recognition by T-cell membrane coating the nanoparticles leads to more specific binding of nanoparticles to tumour cells (Figure 19). Using

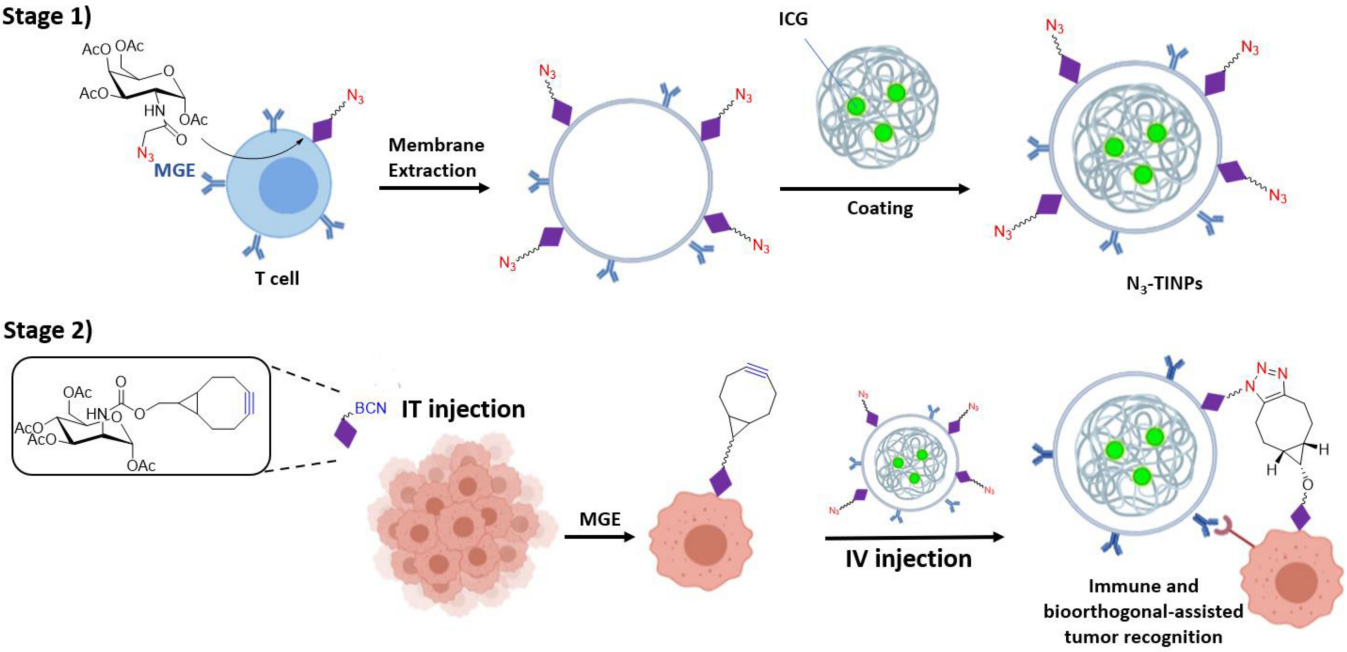

Figure 19. Illustration of the dual targeting mechanism of N_3-labelled T cell membrane-coated ICG-PLGA nanoparticles for photothermal therapy. Stage 1) Azide expression in T-cells through MGE by Ac_4GalNAz and extraction of labelled T-membrane to coat ICG-PLGA polymeric core forming N_3-TINPs. Stage 2) BCN-expression in tumour cells through MGE by IT injection of Ac_4ManNBCN. Bioorthogonal click reaction with the BCN groups beside the T-cell membrane immune reaction, increases recognition and the selectivity of T-cells for the tumour.

nanoparticles alone to deliver the photosensitiser is usually insufficient to achieve the high intensity needed for photothermal therapy.[204] Moreover, using active targeting alone (T-cell immunogenicity recognition) is also generally insufficient due to tumour cells' heterogenicity and non-specific distribution to different body organs.[205] However, the specific MGE of tumour cells' surface glycans was achieved by the intratumour injection of Ac_4ManNBCN which makes it challenging for clinical applications.

4. Two-Step Pretargeting Approach in Radiolabelling

In this section, we focus on the pretargeting cancer radioimaging and therapy approach to highlight its advantages and challenges compared with other direct labelling approaches such as direct conjugation of Abs to radioligands. Pretargeting generally aims to separate the administration of the radionuclide from the mAb, it was first developed in the mid-1980s to overcome the long circulation time that is required for the radiolabelled antibodies (directly attached radionuclides to mAbs) that are used for cancer imaging and therapy.[206] Before using bioorthogonal chemistry to selectively link the mAb with the radionuclide after their two-steps administration, non-covalent interactions like streptavidin-biotin were reported to do the same purpose. An antibody linked with streptavidin is administered first for tumour accumulation followed by a radiolabelled biotin to limit the radioactivity to the tumour site.[207,208] In bioorthogonal approaches, the antibody-bioorthogonal component conjugate is given first to allow sufficient accumulation at the tumour site and clearance of unbound antibodies from the blood and non-tumour tissues. Then, the radioligand (diagnostic or therapeutic conjugated with the second bioorthogonal component) is delivered[209] and the bioorthogonal reaction ensures selectivity (Table 6). Despite the high affinity and fast binding rate ($3x10^6$–$4.5x10^7\ M^{-1}\ s^{-1}$) between the streptavidin–biotin,[210] conjugating the mAb to streptavidin was found to have certain drawbacks. First, it increases accumulation of the mAb in the liver, compromising the chances of effective tumour localisation of the biotin radionuclide.[211] Second, the streptavidin–mAbs have a higher internalisation rate which decreases their availability to react with the biotin. Finally, the streptavidin-mAbs can have immunogenicity.[212] For these reasons, the bioorthogonal click approach is considered a safer and more useful approach. Nanoparticles have also been used to first pretarget the tumour by the EPR effect before the administration of the radionuclide (Table 6). This brings wider applications for solid tumours compared to mAbs which rely on the targeting of specific overexpressed proteins.

In imaging applications, the *in vivo* administration interval between the bioorthogonally tagged mAb and the bioorthogonally tagged radionuclide varies between studies (between 24 and 72 h). For NPs, the administration interval between the bioorthogonally functionalised nanoparticles and the bioorthogonally tagged radionuclide is between 5 minutes and 8 days. This wide range is due to the variation in the accumulation rate of the nanoparticles used for delivery of the first bioorthogonal component. High tumour accumulation is required before administration of the bioorthogonally tagged radionuclide. For theranostic applications, two different bioorthogonally tagged radionuclides are usually used, a diagnostic radioligand for imaging, and a therapeutic radioligand for radioimmunotherapy. The interval between the administration of the three components is critical for the efficiency of both applications. This interval varies from 24-72 h between the administration of the antibody and the diagnostic radioligand. For therapeutic radioligands, the optimum window is usually found to be 24 h as this allows the clearance of the unclicked diagnostic radionuclide so it does not influence the biodistribution of the second radioligand.

The pretargeting strategy has generally improved tumour imaging and radioimmunotherapy by decreasing the background distribution compared to direct targeting. It has also helped to overcome some of the challenges associated with radionuclides where the long half-lives that are required for long term monitoring *in vivo* are associated with slow pharmacokinetic profiles and this usually causes background signals in off-target tissues.[213]

However, none of the TCO-modified Abs or peptides (Table 6) have reached clinical trials to date. The challenges that remain include adjusting the internalisation rates of the mAbs, the radionuclide dose, the modified-Ab tumour accumulation rate, and the clearance rate. Also, as two targeting entities are involved in this two-step approach, their combined adminis-

Table 6. Summary of reported bioorthogonally modified targeting vectors, their complementary imaging and therapeutic radionuclides and the time intervals between their administration in *in vivo* studies.

Targeting vector	Imaging radionuclide	Therapeutic radionuclide	Interval between mAb/nanoparticle and radionuclide	Ref.
MSN-TCO	^{11}C-Tz	–	5 minutes	[170]
Cetuximab-TCO	^{68}Ga-Tz	–	23 h	[158]
THIOMAB-TCO	^{111}In-Tz	–	24 h	[153]
huA33-TCO	^{64}Cu-Tz	^{177}Lu-Tz	24 h	[160]
Anti-CEA 35 A7-TCO	^{177}Lu-Tz	^{177}Lu-Tz	24 h	[162]
Supramolecular nanoparticle-TCO	^{64}Cu-Tz	–	24 h	[171]
CC49-TCO	^{99m}Tc-Tz	–	48 h	[159]
huA33-TCO	^{64}Cu-Tz	^{67}Cu-Tz	72 h	[161]
Nanostars-TCO	^{18}F-Tz	–	72 h	[172]
MSN-DBCO	^{18}F-N_3	–	1-8 days	[173]

tration, toxicity profiles and cumulative doses must be evaluated before clinical studies can commence.

5. Summary and Outlook

Over the past two decades, bioorthogonal click chemistry has emerged as a facile means of studying biomolecules in their native environment in living systems and *in vivo*. In this review, advances in bioorthogonal chemistry-based *in vivo* applications have been summarised according to their chemical mechanism, and the targeting strategy that is used to deliver the bioorthogonal components. Metabolic bioengineering is the mechanism used most often to label cells with bioorthogonal components due to the facile development of bioorthogonally modified monosaccharides, the high metabolic rates of tumour cells, and the lack of toxicity of these unnatural monosaccharides. The main limitation of using metabolic bioengineering for delivering bioorthogonal components in cancer-related applications is the low *in vivo* selectivity. Because these unnatural monosaccharides are building blocks in the biosynthetic pathways of cellular glycans, they can be taken up by non-cancerous cells. This makes metabolic bioengineering more suitable in therapeutic cell-related applications than cancer-related applications, as therapeutic cells first undergo bioorthogonal labelling by metabolic bioengineering *in vitro* before their injection *in vivo*. This eliminates the chances of labelling normal cells.

Active targeting is a more appropriate and selective mechanism for the delivery of bioorthogonal components in cancer-related applications as it depends on specific antigens or receptors for its effectiveness. This targeting mechanism is most often used for cancer radioimaging and radiotherapy applications *in vivo* due to the ease of chemical modification of the antibodies with one bioorthogonal component (i.e., TCO) and modification of the radioligand with the complementary bioorthogonal component (i.e., Tz) without affecting the antibody's immunogenicity. This strategy has been developed to afford pretargeting approaches in which a scheduling gap is introduced between the administration of the bioorthogonal components, to allow clearance of unbound antibodies and hence minimise the background noise. However, optimising this scheduling gap between the two bioorthogonal components, the radioligand dose, and the bioorthogonally modified antibody tumour accumulation and clearance rates is still the main challenge to this strategy, and thus further research *in vivo* is required before this method can be fully translated into the clinic.

Passive targeting is the most convenient delivery mechanism for bioorthogonal components in cancer-related applications owing to its many advantages over MGE and active targeting approaches. As it relies on the EPR effect and not on specific antigens/receptors to deliver components to tumour regions, it can arguably address challenges associated with tumour heterogeneity. It also allows the simultaneous administration of two bioorthogonal components with no time interval needed between them. In this case, each of the bioorthogonal components is enclosed in a nanoparticle, and both nanoparticles are administered at the same time. This makes it a more clinically applicable approach, particularly for prodrug activation applications. However, as passive targeting is mainly dependent on the EPR effect, which is highly affected by tumour type, size and vasculature, the accumulation rates and patient responses can vary extensively.

Using different targeting mechanisms simultaneously has helped to address the challenges of each individual targeting strategy. Combining MGE with passive targeting is advantageous when functionalised to increase the saccharide selectivity and hence the MGE so as to avoid off-site azide expression. It allows the intravenous administration of the modified monosaccharide, which makes it clinically applicable and a better option than using MGE alone for tumour-targeting applications. Combining active with passive targeting resulted in a successful strategy for deep delivery of chemotherapeutic drugs to deep avascular tumour regions. Using passive targeting alone would selectively deliver chemotherapeutic drugs to the tumour site due to the EPR effect. However, this proved insufficient for reaching deep avascular tumour regions meaning alternative approaches would be required there.

The second factor for a successful *in vivo* bioorthogonal-based application is maximising the efficiency of the bioorthogonal reaction itself. Despite the large number of reported bioorthogonal reactions, only a few are applicable *in vivo*. Reactions with fast kinetics are preferred for *in vivo* application (IEDDA ~ 10^4 $M^{-1}s^{-1}$ > CuAAC ~ 10^1 $M^{-1}s^{-1}$ > SPAAC ~ 10^{-1} $M^{-1}s^{-1}$ > Staudinger ligation ~ 10^{-3} $M^{-1}s^{-1}$ > Oxime ligation ~ 10^{-4} $M^{-1}s^{-1}$). The selectivity of the bioorthogonal reaction is also an important factor to be considered. This is because in the *in vivo* environment, there is a high dilution factor compared to the *in vitro* environment, and for translation from *in vitro* models to *in vivo* models and ultimately clinical models, the reaction kinetics to overcome the decrease in target concentration, the reagent's dilution and the reagent's clearance need definite consideration. Using targeting mechanisms such as passive and active targeting also plays a role in decreasing this *in vivo* dilution factor to help amplify the bioorthogonal reaction's selectivity.

In summary, developments with *in vivo* applications of bioorthogonal reactions have improved greatly over the past two decades. As it is still an active research area, the likelihood of further developments is high, thus making it an exciting and impactful area for future clinical applications.

Acknowledgements

The authors acknowledge the Egyptian Ministry of Higher Education and Scientific Research and The British Council (Newton-Mosharafa Fund) represented by the Egyptian Bureau for Cultural and Educational Affairs in London for financial support.

Conflict of Interest

The authors declare no conflict of interest.

Data Availability Statement

Data sharing is not applicable to this article as no new data were created or analyzed in this study.

Keywords: bioorthogonal chemistry · click chemistry · *in vivo* · metabolic glycoengineering

[1] G. Lv, K. Li, L. Qiu, Y. Peng, X. Zhao, X. Li, Q. Liu, S. Wang, J. Lin, *Pharm. Res.* **2018**, *35*, 63
[2] W. Xuan, Y. Xia, T. Li, L. Wang, Y. Liu, W. Tan, *J. Am. Chem. Soc.* **2020**, *142*, 937–944.
[3] Y. Kim, Z. Zhang, J. H. Shim, T. S. Lee, C. H. Tung, *Bioorg. Med. Chem.* **2018**, *26*, 758–764.
[4] Y. R. Kim, Y. H. Kim, S. W. Kim, Y. J. Lee, D. E. Chae, K. A. Kim, Z. W. Lee, N. D. Kim, J. S. Choi, I. S. Choi, K. B. Lee, *Chem. Commun.* **2016**, *52*, 11764–11767.
[5] S. C. H. A. van der Steen, R. Raavé, S. Langerak, L. van Houdt, S. M. J. van Duijnhoven, S. A. M. van Lith, L. F. A. G. Massuger, W. F. Daamen, W. P. Leenders, T. H. van Kuppevelt, *Eur. J. Pharm. Biopharm.* **2017**, *113*, 229–239.
[6] F. Neubert, G. Beliu, U. Terpitz, C. Werner, C. Geis, M. Sauer, S. Doose, *Angew. Chem. Int. Ed.* **2018**, *57*, 16364–16369; *Angew. Chem.* **2018**, *130*, 16602–16607.
[7] T. Tamura, T. Ueda, T. Goto, T. Tsukidate, Y. Shapira, Y. Nishikawa, A. Fujisawa, I. Hamachi, *Nat. Commun.* **2018**, *9*, 1–12.
[8] E. Ros, M. Bellido, X. Verdaguer, L. R. De Pouplana, A. Riera, *Bioconjugate Chem.* **2020**, *31*, 933–938.
[9] C. Baker, T. Rodrigues, B. P. De Almeida, N. L. Barbosa-Morais, G. J. L. Bernardes, *Bioorg. Med. Chem.* **2019**, *27*, 2531–2536.
[10] T. Carell, M. Vrabel, *Top. Curr. Chem.* **2016**, *374*, 1–21.
[11] C. P. Ramil, Q. Lin, *Chem. Commun.* **2013**, *49*, 11007–11022.
[12] A. Borrmann, J. C. M. Van Hest, *Chem. Sci.* **2014**, *5*, 2123–2134.
[13] H. W. Shih, D. N. Kamber, J. A. Prescher, *Curr. Opin. Chem. Biol.* **2014**, *21*, 103–111.
[14] Y. Li, H. Fu, *ChemistryOpen* **2020**, *9*, 835–853.
[15] R. E. Bird, S. A. Lemmel, X. Yu, Q. A. Zhou, *Bioconjugate Chem.* **2021**, *32*, 2457–2479.
[16] L. H. Qin, W. Hu, Y. Q. Long, *Tetrahedron Lett.* **2018**, *59*, 2214–2228.
[17] A. Godinat, A. A. Bazhin, E. A. Goun, *Drug Discovery Today* **2018**, *23*, 1584–1590.
[18] M. K. Rahim, R. Kota, S. Lee, J. B. Haun, *Nanotechnol. Rev.* **2013**, *2*, 215–227.
[19] V. Rigolot, C. Biot, C. Lion, *Angew. Chem. Int. Ed.* **2021**, *60*, 23084–23105; *Angew. Chem.* **2021**, *133*, 23268–23289.
[20] H. C. Hang, C. Yu, D. L. Kato, C. R. Bertozzi, *Proc. Natl. Acad. Sci. USA* **2003**, *100*, 14846–14851.
[21] G. A. Lemieux, C. R. Bertozzi, *Trends Biotechnol.* **1998**, *16*, 506–513.
[22] L. K. Mahal, K. J. Yarema, C. R. Bertozzi, *Science* **1997**, *276*, 1125–1128.
[23] K. Severinov, T. W. Muir, *J. Biol. Chem.* **1998**, *273*, 16205–16209.
[24] E. Saxon, J. I. Armstrong, C. R. Bertozzi, *Org. Lett.* **2000**, *2*, 2141–2143.
[25] E. Saxon, C. R. Bertozzi, *Science* **2000**, *287*, 2007–2010.
[26] V. V. Rostovtsev, L. G. Green, V. V. Fokin, K. B. Sharpless, *Angew. Chem. Int. Ed.* **2002**, *41*, 2596–2599; *Angew. Chem.* **2002**, *114*, 2708–2711.
[27] M. Schnölzer, S. B. H. Kent, *Science* **1992**, *256*, 221–225.
[28] T. W. Muir, M. J. Williams, M. H. Ginsberg, S. B. H. Kent, *Biochemistry* **1994**, *33*, 7701–7708.
[29] T. W. Muir, *Structure* **1995**, *3*, 649–652.
[30] T. W. Muir, P. E. Dawson, S. B. H. Kent, *Methods Enzymol.* **1997**, *289*, 266–298.
[31] M. A. Walker, *Angew. Chem. Int. Ed. Engl.* **1997**, *36*, 1069–1071.
[32] Y. Bai, J. Chen, S. C. Zimmerman, *Chem. Soc. Rev.* **2018**, *47*, 1811–1821.
[33] B. L. Nilsson, L. L. Kiessling, R. T. Raines, *Org. Lett.* **2000**, *2*, 1939–1941.
[34] M. Azoulay, G. Tuffin, W. Sallem, J. C. Florent, *Bioorg. Med. Chem. Lett.* **2006**, *16*, 3147–3149.
[35] R. Van Brakel, R. C. M. Vulders, R. J. Bokdam, H. Grüll, M. S. Robillard, *Bioconjugate Chem.* **2008**, *19*, 714–718.
[36] F. L. Lin, H. M. Hoyt, H. Van Halbeek, R. G. Bergman, C. R. Bertozzi, *J. Am. Chem. Soc.* **2005**, *127*, 2686–2695.
[37] M. Sundhoro, S. Jeon, J. Park, O. Ramström, M. Yan, *Angew. Chem. Int. Ed.* **2017**, *56*, 12117–12121; *Angew. Chem.* **2017**, *129*, 12285–12289.
[38] M. J. Hangauer, C. R. Bertozzi, *Angew. Chem. Int. Ed.* **2008**, *47*, 2394–2397; *Angew. Chem.* **2008**, *120*, 2428–2431.
[39] L. Cheng, X. Kang, D. Wang, Y. Gao, L. Yi, Z. Xi, *Org. Biomol. Chem.* **2019**, *17*, 5675–5679.
[40] A. S. Cohen, E. A. Dubikovskaya, J. S. Rush, C. R. Bertozzi, *J. Am. Chem. Soc.* **2010**, *132*, 8563–8565.
[41] J. B. Pawlak, G. P. P. Gential, T. J. Ruckwardt, J. S. Bremmers, N. J. Meeuwenoord, F. A. Ossendorp, H. S. Overkleeft, D. V. Filippov, S. I. Van Kasteren, *Angew. Chem. Int. Ed.* **2015**, *54*, 5628–5631; *Angew. Chem.* **2015**, *127*, 5720–5723.
[42] J. Luo, Q. Liu, K. Morihiro, A. Deiters, *Nat. Chem.* **2016**, *8*, 1027–1034.
[43] M. Fottner, A.-D. Brunner, V. Bittl, D. Horn-Ghetko, A. Jussupow, V. R. I. Kaila, A. Bremm, K. Lang, *Nat. Chem. Biol.* **2019**, *15*, 276–284.
[44] M. Mondal, R. Liao, L. Xiao, T. Eno, J. Guo, *Angew. Chem. Int. Ed.* **2017**, *56*, 2636–2639; *Angew. Chem.* **2017**, *129*, 2680–2683.
[45] J. A. Prescher, D. H. Dube, C. R. Bertozzi, *Nature* **2004**, *430*, 873–877.
[46] L. Shah, S. T. Laughlin, I. S. Carrico, *J. Am. Chem. Soc.* **2016**, *138*, 5186–5189.
[47] P. Zhang, X. Zhang, C. Li, S. Zhou, W. Wu, X. Jiang, *ACS Appl. Mater. Interfaces* **2019**, *11*, 32697–32705.
[48] K. J. Yarema, L. K. Mahal, R. E. Bruehl, E. C. Rodriguez, C. R. Bertozzi, *J. Biol. Chem.* **1998**, *273*, 31168–31179.
[49] D. A. Nauman, C. R. Bertozzi, *Biochim. Biophys. Acta Gen. Subj.* **2001**, *1568*, 147–154.
[50] K. Lang, J. W. Chin, *Chem. Rev.* **2014**, *114*, 4764–4806.
[51] H. D. King, G. M. Dubowchik, H. Mastalerz, D. Willner, S. J. Hofstead, R. A. Firestone, S. J. Lasch, P. A. Trail, *J. Med. Chem.* **2002**, *45*, 4336–4343.
[52] D. Dutta, A. Pulsipher, W. Luo, M. N. Yousaf, *J. Am. Chem. Soc.* **2011**, *133*, 8704–8713.
[53] Y. Zeng, T. N. C. Ramya, A. Dirksen, P. E. Dawson, J. C. Paulson, *Nat. Methods* **2009**, *6*, 207–209.
[54] S. Wang, G. N. Nawale, S. Kadekar, O. P. Oommen, N. K. Jena, S. Chakraborty, J. Hilborn, O. P. Varghese, *Sci. Rep.* **2018**, *8*, 1–7.
[55] M. Rashidian, M. M. Mahmoodi, R. Shah, J. K. Dozier, C. R. Wagner, M. D. Distefano, *Bioconjugate Chem.* **2013**, *24*, 333–342.
[56] Y. Xu, L. Xu, Y. Xia, C. J. Guan, Q. X. Guo, Y. Fu, C. Wang, Y. M. Li, *Chem. Commun.* **2015**, *51*, 13189–13192.
[57] P. Schmidt, C. Stress, D. Gillingham, *Chem. Sci.* **2015**, *6*, 3329–3333.
[58] L. Tang, Q. Yin, Y. Xu, Q. Zhou, K. Cai, J. Yen, L. W. Dobrucki, J. Cheng, *Chem. Sci.* **2015**, *6*, 2182–2186.
[59] I. Fur, O. Chemie, D. E. R. U. Munchen, *Angew. Chem. Int. Ed.* **1963**, *2*, 633–696; *Angew. Chem.* **1963**, *75*, 742–754.
[60] C. W. Tornøe, C. Christensen, M. Meldal, *J. Org. Chem.* **2002**, *67*, 3057–3064.
[61] D. C. Kennedy, C. S. McKay, M. C. B. Legault, D. C. Danielson, J. A. Blake, A. F. Pegoraro, A. Stolow, Z. Mester, J. P. Pezacki, *J. Am. Chem. Soc.* **2011**, *133*, 17993–18001.
[62] S. Li, H. Cai, J. He, H. Chen, S. Lam, T. Cai, Z. Zhu, S. J. Bark, C. Cai, *Bioconjugate Chem.* **2016**, *27*, 2315–2322.
[63] T. R. Chan, R. Hilgraf, K. B. Sharpless, V. V. Fokin, *Org. Lett.* **2004**, *6*, 2853–2855.
[64] D. Soriano Del Amo, W. Wang, H. Jiang, C. Besanceney, A. C. Yan, M. Levy, Y. Liu, F. L. Marlow, P. Wu, *J. Am. Chem. Soc.* **2010**, *132*, 16893–16899.
[65] C. Uttamapinant, A. Tangpeerachaikul, S. Grecian, S. Clarke, U. Singh, P. Slade, K. R. Gee, A. Y. Ting, *Angew. Chem. Int. Ed.* **2012**, *51*, 5852–5856; *Angew. Chem.* **2012**, *124*, 5954–5958.
[66] F. Wang, Y. Zhang, Z. Liu, Z. Du, L. Zhang, J. Ren, X. Qu, *Angew. Chem. Int. Ed.* **2019**, *58*, 6987–6992; *Angew. Chem.* **2019**, *131*, 7061–7066.
[67] J. Clavadetscher, S. Hoffmann, A. Lilienkampf, L. Mackay, R. M. Yusop, S. A. Rider, J. J. Mullins, M. Bradley, *Angew. Chem. Int. Ed.* **2016**, *55*, 15662–15666; *Angew. Chem.* **2016**, *128*, 15891–15895.
[68] N. J. Agard, J. A. Prescher, C. R. Bertozzi, *J. Am. Chem. Soc.* **2004**, *126*, 15046–15047.
[69] J. M. Baskin, J. A. Prescher, S. T. Laughlin, N. J. Agard, P. V. Chang, I. A. Miller, A. Lo, J. A. Codelli, C. R. Bertozzi, *Proc. Natl. Acad. Sci. USA* **2007**, *104*, 16793–16797.

[70] J. A. Codelli, J. M. Baskin, N. J. Agard, C. R. Bertozzi, *J. Am. Chem. Soc.* **2008**, *130*, 11486–11493.
[71] N. J. Agard, J. M. Baskin, J. A. Prescher, A. Lo, C. R. Bertozzi, *ACS Chem. Biol.* **2006**, *1*, 644–648.
[72] N. E. Mbua, J. Guo, M. A. Wolfert, R. Steet, G. J. Boons, *ChemBioChem* **2011**, *12*, 1912–1921.
[73] J. Dommerholt, S. Schmidt, R. Temming, L. J. A. Hendriks, F. P. J. T. Rutjes, J. C. M. Van Hest, D. J. Lefeber, P. Friedl, F. L. Van Delft, *Angew. Chem. Int. Ed.* **2010**, *49*, 9422–9425; *Angew. Chem.* **2010**, *122*, 9612–9615.
[74] J. C. Jewett, E. M. Sletten, C. R. Bertozzi, *J. Am. Chem. Soc.* **2010**, *132*, 3688–3690.
[75] T. Plass, S. Milles, C. Koehler, C. Schultz, E. A. Lemke, *Angew. Chem. Int. Ed.* **2011**, *50*, 3878–3881; *Angew. Chem.* **2011**, *123*, 3964–3967.
[76] S. Song, M. K. Shim, S. Lim, Y. Moon, S. Yang, J. Kim, Y. Hong, H. Y. Yoon, I. S. Kim, K. Y. Hwang, K. Kim, *Bioconjugate Chem.* **2020**, *31*, 1562–1574.
[77] H. I. Yoon, J. Y. Yhee, J. H. Na, S. Lee, H. Lee, S. Kang, K. Kim, **2016**, 10.1021/acs.bioconjchem.6b00010.
[78] N. Liao, D. Zhang, M. Wu, H. Yang, X. Liu, J. Song, *Nanoscale* **2021**, 10.1039/d0nr07272a.
[79] K. C. Rui Huang, Peter S. Conti, *Methods Mol. Biol.* **2016**, *1444*, 73–84.
[80] K. J. Shea, J. S. Kim, *J. Am. Chem. Soc.* **1992**, *114*, 4846–4855.
[81] S. S. Matikonda, D. L. Orsi, V. Staudacher, I. A. Jenkins, F. Fiedler, J. Chen, A. B. Gamble, *Chem. Sci.* **2015**, *6*, 1212–1218.
[82] Y. Ge, X. Fan, P. R. Chen, *Chem. Sci.* **2016**, *7*, 7055–7060.
[83] J. M. Fairhall, J. C. Camilli, B. H. Gibson, S. Hook, A. B. Gamble, *Bioorg. Med. Chem.* **2021**, *46*, 116361.
[84] K. Kodama, S. Fukuzawa, H. Nakayama, T. Kigawa, K. Sakamoto, T. Yabuki, N. Matsuda, M. Shirouzu, K. Takio, K. Tachibana, S. Yokoyama, *ChemBioChem* **2006**, *7*, 134–139.
[85] K. Kodama, S. Fukuzawa, H. Nakayama, K. Sakamoto, T. Kigawa, T. Yabuki, N. Matsuda, M. Shirouzu, K. Takio, S. Yokoyama, K. Tachibana, *ChemBioChem* **2007**, *8*, 232–238.
[86] G. Guo, X. Sun, C. Chen, S. Wu, P. Huang, Z. Li, M. Dean, Y. Huang, W. Jia, Q. Zhou, A. Tang, Z. Yang, X. Li, P. Song, X. Zhao, R. Ye, S. Zhang, Z. Lin, M. Qi, S. Wan, L. Xie, F. Fan, M. L. Nickerson, X. Zou, X. Hu, L. Xing, Z. Lv, H. Mei, S. Gao, C. Liang, Z. Gao, J. Lu, Y. Yu, C. Liu, L. Li, X. Fang, Z. Jiang, J. Yang, C. Li, X. Zhao, J. Chen, F. Zhang, Y. Lai, Z. Lin, F. Zhou, H. Chen, H. C. Chan, S. Tsang, D. Theodorescu, Y. Li, X. Zhang, J. Wang, H. Yang, Y. Gui, J. Wang, Z. Cai, *Nat. Genet.* **2013**, *45*, 1459–1463.
[87] J. M. Chalker, C. S. C. Wood, B. G. Davis, *J. Am. Chem. Soc.* **2009**, *131*, 16346–16347.
[88] B. Rubio-Ruiz, J. T. Weiss, A. Unciti-Broceta, *J. Med. Chem.* **2016**, *59*, 9974–9980.
[89] J. T. Weiss, J. C. Dawson, C. Fraser, W. Rybski, C. Torres-Sánchez, M. Bradley, E. E. Patton, N. O. Carragher, A. Unciti-Broceta, *J. Med. Chem.* **2014**, *57*, 5395–5404.
[90] R. M. Yusop, A. Unciti-Broceta, E. M. V. Johansson, R. M. Sánchez-Martín, M. Bradley, *Nat. Chem.* **2011**, *3*, 239–243.
[91] M. A. Miller, B. Askevold, H. Mikula, R. H. Kohler, D. Pirovich, R. Weissleder, *Nat. Commun.* **2017**, *8*, 1–13.
[92] B. Li, P. Liu, H. Wu, X. Xie, Z. Chen, F. Zeng, S. Wu, *Biomaterials* **2017**, *138*, 57–68.
[93] B. L. Oliveira, B. J. Stenton, V. B. Unnikrishnan, C. R. De Almeida, J. Conde, M. Negrão, F. S. S. Schneider, C. Cordeiro, M. G. Ferreira, G. F. Caramori, J. B. Domingos, R. Fior, G. J. L. Bernardes, *J. Am. Chem. Soc.* **2020**, *142*, 10869–10880.
[94] M. L. Blackman, M. Royzen, J. M. Fox, *J. Am. Chem. Soc.* **2008**, *130*, 13518–13519.
[95] N. K. Devaraj, R. Weissleder, S. A. Hilderbrand, *Bioconjugate Chem.* **2008**, *19*, 2297–2299.
[96] H. Stöckmann, A. A. Neves, S. Stairs, K. M. Brindle, F. J. Leeper, *Org. Biomol. Chem.* **2011**, *9*, 7303–7305.
[97] S. Stairs, A. A. Neves, H. Stöckmann, Y. A. Wainman, H. Ireland-Zecchini, K. M. Brindle, F. J. Leeper, *ChemBioChem* **2013**, *14*, 1063–1067.
[98] J. Tu, M. Xu, S. Parvez, R. T. Peterson, R. M. Franzini, *J. Am. Chem. Soc.* **2018**, *140*, 8410–8414.
[99] J. Tu, D. Svatunek, S. Parvez, H. J. Eckvahl, M. Xu, R. T. Peterson, K. N. Houk, R. M. Franzini, *Chem. Sci.* **2020**, *11*, 169–179.
[100] R. Selvaraj, J. M. Fox, *Curr. Opin. Chem. Biol.* **2013**, *17*, 753–760.
[101] M. T. Taylor, M. L. Blackman, O. Dmitrenko, J. M. Fox, *J. Am. Chem. Soc.* **2011**, *133*, 9646–9649.
[102] D. N. Kamber, L. A. Nazarova, Y. Liang, S. A. Lopez, D. M. Patterson, H. W. Shih, K. N. Houk, J. A. Prescher, *J. Am. Chem. Soc.* **2013**, *135*, 13680–13683.
[103] J. M. J. M. Ravasco, C. M. Monteiro, A. F. Trindade, *Org. Chem. Front.* **2017**, *4*, 1167–1198.
[104] S. B. Engelsma, L. I. Willems, C. E. Van Paaschen, S. I. Van Kasteren, G. A. Van Der Marel, H. S. Overkleeft, D. V. Filippov, *Org. Lett.* **2014**, *16*, 2744–2747.
[105] S. Eising, F. Lelivelt, K. M. Bonger, *Angew. Chem. Int. Ed.* **2016**, *55*, 12243–12247; *Angew. Chem.* **2016**, *128*, 12431–12435.
[106] I. Dovgan, A. Hentz, O. Koniev, A. Ehkirch, S. Hessmann, S. Ursuegui, S. Delacroix, M. Riomet, F. Taran, S. Cianférani, S. Kolodych, A. Wagner, *Chem. Sci.* **2020**, *11*, 1210–1215.
[107] A. Darko, S. Wallace, O. Dmitrenko, M. M. Machovina, R. A. Mehl, J. W. Chin, J. M. Fox, *Chem. Sci.* **2014**, *5*, 3770–3776.
[108] M. R. Karver, R. Weissleder, S. A. Hilderbrand, *Bioconjugate Chem.* **2011**, *22*, 2263–2270.
[109] D. N. Kamber, Y. Liang, R. J. Blizzard, F. Liu, R. A. Mehl, K. N. Houk, J. A. Prescher, *J. Am. Chem. Soc.* **2015**, *137*, 8388–8391.
[110] R. M. Versteegen, R. Rossin, W. Ten Hoeve, H. M. Janssen, M. S. Robillard, *Angew. Chem. Int. Ed.* **2013**, *52*, 14112–14116; *Angew. Chem.* **2013**, *125*, 14362–14366.
[111] J. Li, S. Jia, P. R. Chen, *Nat. Chem. Biol.* **2014**, *10*, 1003–1005.
[112] L. Zuo, J. Ding, C. Li, F. Lin, P. R. Chen, P. Wang, G. Lu, J. Zhang, L. L. Huang, H. Y. Xie, *Chem. Sci.* **2020**, *11*, 2155–2160.
[113] Q. Yao, F. Lin, X. Fan, Y. Wang, Y. Liu, Z. Liu, X. Jiang, P. R. Chen, Y. Gao, *Nat. Commun.* **2018**, *9*, 1–9.
[114] R. Rossin, S. M. J. Van Duijnhoven, W. Ten Hoeve, H. M. Janssen, L. H. J. Kleijn, F. J. M. Hoeben, R. M. Versteegen, M. S. Robillard, *Bioconjugate Chem.* **2016**, *27*, 1697–1706.
[115] R. Rossin, R. M. Versteegen, J. Wu, A. Khasanov, H. J. Wessels, E. J. Steenbergen, W. Ten Hoeve, H. M. Janssen, A. H. A. M. Van Onzen, P. J. Hudson, M. S. Robillard, *Nat. Commun.* **2018**, *9*, 1–11.
[116] H. Li, J. Conde, A. Guerreiro, G. J. L. Bernardes, *Angew. Chem. Int. Ed.* **2020**, *59*, 16023–16032; *Angew. Chem.* **2020**, *132*, 16157–16166.
[117] G. Zhang, J. Li, R. Xie, X. Fan, Y. Liu, S. Zheng, Y. Ge, P. R. Chen, *ACS Cent. Sci.* **2016**, *2*, 325–331.
[118] A. H. A. M. Van Onzen, R. M. Versteegen, F. J. M. Hoeben, I. A. W. Filot, R. Rossin, T. Zhu, J. Wu, P. J. Hudson, H. M. Janssen, W. Ten Hoeve, M. S. Robillard, *J. Am. Chem. Soc.* **2020**, *142*, 10955–10963.
[119] H. Wu, S. C. Alexander, S. Jin, N. K. Devaraj, *J. Am. Chem. Soc.* **2016**, *138*, 11429–11432.
[120] X. Xie, B. Li, J. Wang, C. Zhan, Y. Huang, F. Zeng, S. Wu, *ACS Materials Lett.* **2019**, *1*, 549–557.
[121] X. Xie, B. Li, J. Wang, C. Zhan, Y. Huang, F. Zeng, S. Wu, *ACS Appl. Mater. Interfaces* **2019**, *11*, 41875–41888.
[122] E. Jiménez-Moreno, Z. Guo, B. L. Oliveira, I. S. Albuquerque, A. Kitowski, A. Guerreiro, O. Boutureira, T. Rodrigues, G. Jiménez-Osés, G. J. L. Bernardes, *Angew. Chem. Int. Ed.* **2017**, *56*, 243–247; *Angew. Chem.* **2017**, *129*, 249–253.
[123] K. Neumann, A. Gambardella, A. Lilienkampf, M. Bradley, *Chem. Sci.* **2018**, *9*, 7198–7203.
[124] J. Dong, L. Krasnova, M. G. Finn, K. Barry Sharpless, *Angew. Chem. Int. Ed.* **2014**, *53*, 9430–9448; *Angew. Chem.* **2014**, *126*, 9584–9603.
[125] Z. Liu, J. Li, S. Li, G. Li, K. B. Sharpless, P. Wu, *J. Am. Chem. Soc.* **2018**, *140*, 2919–2925.
[126] Q. Li, Q. Chen, P. C. Klauser, M. Li, F. Zheng, N. Wang, X. Li, Q. Zhang, X. Fu, Q. Wang, Y. Xu, L. Wang, *Cell* **2020**, *182*, 85–97.e16.
[127] H. Zhang, Y. Han, Y. Yang, F. Lin, K. Li, L. Kong, H. Liu, Y. Dang, J. Lin, P. R. Chen, *J. Am. Chem. Soc.* **2021**, *143*, 16377–16382.
[128] Y. Han, Z. Yang, H. Hu, H. Zhang, L. Chen, K. Li, L. Kong, Q. Wang, B. Liu, M. Wang, J. Lin, P. R. Chen, *J. Am. Chem. Soc.* **2022**, *144*, 5702–5707.
[129] A. F. Hadfield, S. L. Mella, A. C. Sartorelli, *J. Pharm. Sci.* **1983**, *72*, 748–751.
[130] H. J. Gross, R. Brossmer, *Eur. J. Biochem.* **1988**, *177*, 583–589.
[131] H. J. Groß, R. Brossmer, *Glycoconjugate J.* **1995**, *12*, 739–746.
[132] J. Du, M. A. Meledeo, Z. Wang, H. S. Khanna, V. D. P. Paruchuri, K. J. Yarema, *Glycobiology* **2009**, *19*, 1382–1401.
[133] C. Agatemor, M. J. Buettner, R. Ariss, K. Muthiah, C. T. Saeui, K. J. Yarema, *Nat. Chem. Rev.* **2019**, *3*, 605–620.
[134] M. Gutmann, J. Bechold, J. Seibel, L. Meinel, T. Lühmann, *ACS Biomater. Sci. Eng.* **2019**, *5*, 215–233.
[135] J. E. G. A. Dold, V. Wittmann, *ChemBioChem* **2020**, *22*, 1243–1251.
[136] Y. Iwasaki, H. Maie, K. Akiyoshi, *Biomacromolecules* **2007**, *8*, 3162–3168.

[137] P. R. Wratil, R. Horstkorte, W. Reutter, *Angew. Chem. Int. Ed.* **2016**, *55*, 9482–9512; *Angew. Chem.* **2016**, *128*, 9632–9665.
[138] A. M. Jawalekar, S. Malik, J. M. M. Verkade, B. Gibson, N. S. Barta, J. C. Hodges, A. Rowan, F. L. Van Delft, *Molecules* **2013**, *18*, 7346–7363.
[139] J. C. Jewett, C. R. Bertozzi, *Chem. Soc. Rev.* **2010**, *39*, 1272–1279.
[140] C. S. Lin, Z. C. Xin, J. Dai, T. F. Lue, *Histol. Histopathol.* **2013**, *28*, 1109–1116.
[141] S. Lim, H. Yeol, S. Park, S. Song, M. Kyu, S. Yang, S. Kang, D. Lim, B. Kim, S. Moon, *Biomaterials* **2021**, *266*, 120472.
[142] X. Liu, F. Wu, K. Cai, Z. Zhao, Z. Zhang, Y. Chen, Y. Liu, J. Cheng, L. Yin, *Biomater. Sci.* **2021**, *9*, 1301–1312.
[143] D. W. S. Dhivya, R. Sudhan, *Pharmacol. Ther.* **2015**, *155*, 105–116.
[144] J. H. Jang, H. Lee, A. Sharma, S. M. Lee, T. H. Lee, C. Kang, J. S. Kim, *Chem. Commun.* **2016**, *52*, 9965–9968.
[145] P. Zhang, B. Dong, E. Zeng, F. Wang, Y. Jiang, D. Li, D. Liu, P. Zhang, B. Dong, E. Zeng, F. Wang, Y. Jiang, D. Li, *Anal. Chem.* **2018**, *90*, 11273–11279.
[146] M. F. Barginear, V. John, D. R. Budman, *Mol. Med.* **2012**, *18*, 1473–1479.
[147] R. Haubner, W. A. Weber, A. J. Beer, E. Vabuliene, D. Reim, M. Sarbia, K. F. Becker, M. Goebel, R. Hein, H. J. Wester, H. Kessler, M. Schwaiger, *PLoS Med.* **2005**, *2*, 0244–0252.
[148] R. Luria-Pérez, G. Helguera, J. A. Rodríguez, *Bol. Med. Hosp. Infant. Mex.* **2016**, *73*, 372–379.
[149] J. A. Ledermann, S. Canevari, T. Thigpen, *Ann. Oncol.* **2015**, *26*, 2034–2043.
[150] S. Awwad, U. Angkawinitwong, *Pharmaceutica* **2018**, *10*, 1–24.
[151] Z. Chen, R. K. Kankala, Z. Yang, W. Li, S. Xie, H. Li, A. Z. Chen, L. Zou, *Theranostics* **2022**, *12*, 3719–3746.
[152] D. E. Milenic, E. D. Brady, M. W. Brechbiel, *Nat. Rev. Drug Discovery* **2004**, *3*, 488–498.
[153] V. F. C. Ferreira, B. L. Oliveira, A. D'Onofrio, C. M. Farinha, L. Gano, A. Paulo, G. J. L. Bernardes, F. Mendes, *Bioconjugate Chem.* **2021**, *32*, 121–132.
[154] V. Boudousq, L. Bobyk, M. Busson, V. Garambois, M. Jarlier, P. Charalambatou, A. Pèlegrin, S. Paillas, N. Chouin, F. Quenet, P. Maquaire, J. Torgue, I. Navarro-Teulon, J. P. Pouget, *PLoS One* **2013**, *8*, e69613.
[155] A. Maisonial-Besset, T. Witkowski, I. Navarro-Teulon, O. Berthier-Vergnes, G. Fois, Y. Zhu, S. Besse, O. Bawa, A. Briat, M. Quintana, A. Pichard, M. Bonnet, E. Rubinstein, J. P. Pouget, P. Opolon, L. Maigne, E. Miot-Noirault, J. M. Chezal, C. Boucheix, F. Degoul, *Oncotarget* **2017**, *8*, 22034–22047.
[156] R. Rossin, S. M. Van Den Bosch, W. Ten Hoeve, M. Carvelli, R. M. Versteegen, J. Lub, M. S. Robillard, *Bioconjugate Chem.* **2013**, *24*, 1210–1217.
[157] X. Zhang, B. Wang, N. Zhao, Z. Tian, Y. Dai, Y. Nie, J. Tian, Z. Wang, X. Chen, *Theranostics* **2017**, *7*, 20912.
[158] H. L. Evans, Q. D. Nguyen, L. S. Carroll, M. Kaliszczak, F. J. Twyman, A. C. Spivey, E. O. Aboagye, *Chem. Commun.* **2014**, *50*, 9557–9560.
[159] M. F. García, X. Zhang, M. Shah, J. Newton-Northup, P. Cabral, H. Cerecetto, T. Quinn, *Bioorg. Med. Chem.* **2016**, *24*, 1209–1215.
[160] O. Keinänen, J. M. Brennan, R. Membreno, K. Fung, K. Gangangari, E. J. Dayts, C. J. Williams, B. M. Zeglis, *Mol. Pharm.* **2019**, *16*, 4416–4421.
[161] O. Keinänen, K. Fung, J. M. Brennan, N. Zia, M. Harris, E. van Dam, C. Biggin, A. Hedt, J. Stoner, P. S. Donnelly, J. S. Lewis, B. M. Zeglis, *Proc. Natl. Acad. Sci. USA* **2020**, *117*, 28316–28327.
[162] A. Rondon, S. Schmitt, A. Briat, N. Ty, L. Maigne, M. Quintana, R. Membreno, B. M. Zeglis, I. Navarro-Teulon, J. P. Pouget, J. M. Chezal, E. Miot-Noirault, E. Moreau, F. Degoul, *Theranostics* **2019**, *9*, 6706–6718.
[163] A. Rondon, N. Ty, J. B. Bequignat, M. Quintana, A. Briat, T. Witkowski, B. Bouchon, C. Boucheix, E. Miot-Noirault, J. P. Pouget, J. M. Chezal, I. Navarro-Teulon, E. Moreau, F. Degoul, *Sci. Rep.* **2017**, *7*, 1–11.
[164] A. Zlitni, M. Yin, N. Janzen, S. Chatterjee, A. Lisok, K. L. Gabrielson, S. Nimmagadda, M. G. Pomper, F. S. Foster, J. F. Valliant, *PLoS One* **2017**, *12*, 1–17.
[165] T. Dunlap, Y. Cao, *Front. Pharmacol.* **2022**, *13*, 1–12.
[166] H. Modjtahedi, S. Ali, S. Essapen, *Br. Med. Bull.* **2012**, *104*, 41–59.
[167] J. Fang, H. Nakamura, H. Maeda, *Adv. Drug Delivery Rev.* **2011**, *63*, 136–151.
[168] V. Torchilin, *Adv. Drug Delivery Rev.* **2011**, *63*, 131–135.
[169] M. F. Attia, N. Anton, J. Wallyn, Z. Omran, T. F. Vandamme, *J. Pharm. Pharmacol.* **2019**, *71*, 1185–1198.
[170] C. Denk, D. Svatunek, S. Mairinger, J. Stanek, T. Filip, D. Matscheko, C. Kuntner, T. Wanek, H. Mikula, *Bioconjugate Chem.* **2016**, *27*, 1707–1712.
[171] S. Hou, J. S. Choi, M. A. Garcia, Y. Xing, K. J. Chen, Y. M. Chen, Z. K. Jiang, T. Ro, L. Wu, D. B. Stout, J. S. Tomlinson, H. Wang, K. Chen, H. R. Tseng, W. Y. Lin, *ACS Nano* **2016**, *10*, 1417–1424.
[172] J. A. C. M. Goos, M. Davydova, T. R. Dilling, A. Cho, M. A. Cornejo, A. Gupta, W. S. Price, S. Puttick, M. R. Whittaker, J. F. Quinn, T. P. Davis, J. S. Lewis, *Nucl. Med. Biol.* **2020**, *84–85*, 63–72.
[173] H. J. Jeong, R. J. Yoo, J. K. Kim, M. H. Kim, S. H. Park, H. Kim, J. W. Lim, S. H. Do, K. C. Lee, Y. J. Lee, D. W. Kim, *Biomaterials* **2019**, *199*, 32–39.
[174] L. Wang, P. Jing, J. Tan, C. Liao, Y. Chen, Y. Yu, S. Zhang, *Biomaterials* **2021**, *273*, 120823.
[175] J. W. Nichols, Y. H. Bae, *J. Controlled Release* **2014**, *190*, 451–464.
[176] A. Wicki, D. Witzigmann, V. Balasubramanian, J. Huwyler, *J. Controlled Release* **2015**, *200*, 138–157.
[177] F. Danhier, *J. Controlled Release* **2016**, *244*, 108–121.
[178] D. Rosenblum, N. Joshi, W. Tao, J. M. Karp, D. Peer, *Nat. Commun.* **2018**, *9*, 1410.
[179] M. Garcia-Barros, F. Paris, C. Cordon-Cardo, D. Lyden, S. Rafii, A. Haimovitz-Friedman, Z. Fuks, R. Kolesnick, *Science* **2003**, *300*, 1155–1159.
[180] M. Regenold, P. Bannigan, J. C. Evans, A. Waspe, M. J. Temple, C. Allen, *Nanomed. Nanotechnol. Biol. Med.* **2022**, *40*, 102484.
[181] P. De la Torre, M. J. Pérez-Lorenzo, Á. Alcázar-Garrido, A. I. Flores, *Molecules* **2020**, *25*, 10.3390/molecules25030715.
[182] J. Fang, W. Islam, H. Maeda, *Adv. Drug Delivery Rev.* **2020**, *157*, 142–160.
[183] J. Wang, Y. Li, G. Nie, *Nat. Rev. Mater.* **2021**, *6*, 766–783.
[184] J. Park, Y. Choi, H. Chang, W. Um, J. H. Ryu, I. C. Kwon, *Theranostics* **2019**, *9*, 8073–8090.
[185] J. Wu, T. Sun, C. Yang, T. Lv, Y. Bi, Y. Xu, Y. Ling, J. Zhao, R. Cong, Y. Zhang, J. Wang, H. Wen, H. Jiang, F. Li, Z. Huang, *Biomater. Sci.* **2021**, *9*, 1816–1825.
[186] Q. He, Z. Zhang, F. Gao, Y. Li, J. Shi, *Small* **2011**, *7*, 271–280.
[187] K. Wu, N. A. Yee, S. Srinivasan, A. Mahmoodi, M. Zakharian, J. M. Mejia Oneto, M. Royzen, *Chem. Sci.* **2021**, *12*, 1259–1271.
[188] S. Srinivasan, N. A. Yee, K. Wu, M. Zakharian, A. Mahmoodi, M. Royzen, J. M. Mejía Oneto, *Adv. Ther.* **2021**, *4*, 1–11.
[189] K. Greish, *Methods Mol. Biol.* **2010**, *624*, 25–37.
[190] S. Lee, S. Jung, H. Koo, J. H. Na, H. Y. Yoon, M. K. Shim, J. Park, J. H. Kim, S. Lee, M. G. Pomper, I. C. Kwon, C. H. Ahn, K. Kim, *Biomaterials* **2017**, *148*, 1–15.
[191] R. Xie, L. Dong, Y. Du, Y. Zhu, R. Hua, C. Zhang, X. Chen, *Proc. Natl. Acad. Sci. USA* **2016**, *113*, 5173–5178.
[192] A. Shajahan, S. Parashar, S. Goswami, S. Meheboob, N. Perumal, S. Sampathkumar, *J. Am. Chem. Soc.* **2016**, *139*, 693–700.
[193] H. Y. Yoon, M. L. Shin, M. K. Shim, S. Lee, J. H. Na, H. Koo, H. Lee, J. H. Kim, K. Y. Lee, K. Kim, I. C. Kwon, *Mol. Pharm.* **2017**, *14*, 1558–1570.
[194] J. Qiao, F. Tian, Y. Deng, Y. Shang, S. Chen, E. Chang, J. Yao, *Theranostics* **2020**, *10*, 5305–5321.
[195] S. Lee, H. I. Yoon, J. H. Na, S. Jeon, S. Lim, H. Koo, S. S. Han, S. W. Kang, S. J. Park, S. H. Moon, J. H. Park, Y. W. Cho, B. S. Kim, S. K. Kim, T. Lee, D. Kim, S. Lee, M. G. Pomper, I. C. Kwon, K. Kim, *Biomaterials* **2017**, *139*, 12–29.
[196] S. Lim, H. Y. Yoon, H. J. Jang, S. Song, W. Kim, J. Park, K. E. Lee, S. Jeon, S. Lee, D. K. Lim, B. S. Kim, D. E. Kim, K. Kim, *ACS Nano* **2019**, *13*, 10991–11007.
[197] L. Du, H. Qin, T. Ma, T. Zhang, D. Xing, *ACS Nano* **2017**, *11*, 8930–8943.
[198] W. Kim, H. Y. Yoon, S. Lim, P. S. Stayton, I. S. Kim, K. Kim, I. C. Kwon, *J. Controlled Release* **2021**, *329*, 223–236.
[199] H. Pan, W. Li, Z. Chen, Y. Luo, W. He, M. Wang, X. Tang, H. He, L. Liu, M. Zheng, X. Jiang, T. Yin, R. Liang, Y. Ma, L. Cai, *Bioact. Mater.* **2021**, *6*, 951–962.
[200] S. H. Lee, O. K. Park, J. Kim, K. Shin, C. G. Pack, K. Kim, G. Ko, N. Lee, S. H. Kwon, T. Hyeon, *J. Am. Chem. Soc.* **2019**, *141*, 13829–13840.
[201] J. Pellico, I. Fernández-Barahona, M. Benito, Á. Gaitán-Simón, L. Gutiérrez, J. Ruiz-Cabello, F. Herranz, *Nanomed. Nanotechnol. Biol. Med.* **2019**, *17*, 26–35.
[202] M. K. Khang, A. E. Kuriakose, T. Nguyen, C. M. D. Co, J. Zhou, T. T. D. Truong, K. T. Nguyen, L. Tang, *ACS Biomater. Sci. Eng.* **2020**, *6*, 6831–6841.
[203] Y. Han, H. Pan, W. Li, Z. Chen, A. Ma, T. Yin, R. Liang, F. Chen, Y. Ma, Y. Jin, M. Zheng, B. Li, L. Cai, *Adv. Sci.* **2019**, *6*, 1–9.
[204] D. De Melo-Diogo, C. Pais-Silva, D. R. Dias, A. F. Moreira, I. J. Correia, *Adv. Healthcare Mater.* **2017**, *6*, 1700073.
[205] Y. Zhu, J. Feijen, Z. Zhong, *Nano Today* **2018**, *18*, 65–85.

[206] D. Goodwin, C. Meares, C. Diamanti, M. McCall, C. Lai, F. Torti, M. McTigue, B. Martin, *Eur. J. Nucl. Med.* **1984**, *9*, 209–215.
[207] D. B. Axworthy, J. M. Reno, M. D. Hylarides, R. W. Mallett, L. J. Theodore, L. M. Gustavson, F. Su, L. J. Hobson, P. L. Beaumier, A. R. Fritzberg, *Proc. Natl. Acad. Sci. USA* **2000**, *97*, 1802–1807.
[208] M. Zhang, Z. Zhang, K. Garmestani, J. Schultz, D. B. Axworthy, C. K. Goldman, M. W. Brechbiel, J. A. Carrasquillo, T. A. Waldmann, *Proc. Natl. Acad. Sci. USA* **2003**, *100*, 1891–1895.
[209] D. A. Goodwin, C. F. Meares, M. J. Mccall, M. Mctigue, *Eur. J. Nucl. Med.* **1987**, 226–234.
[210] M. Srisa-Art, E. C. Dyson, A. J. DeMello, J. B. Edel, *Anal. Chem.* **2008**, *80*, 7063–7067.
[211] S. Dou, J. Virostko, M. Rusckowski, D. L. Greiner, A. C. Powers, G. Liu, *Front. Pharmacol.* **2014**, *5*, 10.3389/fphar.2014.00172.
[212] V. R. Muzykantov, M. Christofidou-Solomidou, I. Balyasnikova, D. W. Harshaw, L. Schultz, A. B. Fisher, S. M. Albelda, *Proc. Natl. Acad. Sci. USA* **1999**, *96*, 2379–2384.
[213] S. M. Ametamey, M. Honer, P. A. Schubiger, *Chem. Rev.* **2008**, *108*, 1501–1516.

Manuscript received: December 16, 2022
Accepted manuscript online: January 19, 2023
Version of record online: March 2, 2023